FINITE ELEMENT ANALYSIS FOR CONSOLIDATION OF MULTILAYERED AND ANISOTROPIC SOILS

by

Spelios A. Asproudas

Thesis submitted to the Graduate Faculty of the
Virginia Polytechnic Institute and State University
in partial fulfillment of the requirements for the degree of
MASTER OF SCIENCE

in

Civil Engineering

APPROVED:

C. S. Desai, Chairman

R. D. Walker

J. H. Hunter

May, 1975

Blacksburg, Virginia

ACKNOWLEDGEMENTS

The author wishes to express his most heartfelt thanks to Dr. C. S. Desai, for his constant encouragement, prudent guidance and constructive criticism in the preparation of this thesis; and the Department of Civil Engineering for providing a Graduate Teaching Assistantship without which the author could have not continued his education.

In addition, the author is grateful to his parents for their moral support during the past years and to Ginny Newell for typing this thesis.

TABLE OF CONTENTS

LIST OF FIGURES

LIST OF FIGURES, (cont.)

LIST OF FIGURES, (cont.)

Chapter One

INTRODUCTION

Problem Statement

When a soil mass saturated with water is subjected to a compressive load, there is a volume decrease that causes the excess water to drain out, with consequent decrease in the water content; the volumetric decrease of the soil skeleton can be assumed to be negligible. The gradual process of compression of soil as a result of decreasing the water content is called consolidation. Terzaghi [31]* was the first to analyze the phenomenon of consolidation, and his one-dimensional (1-D) theory has since played an important role in modern soil mechanics.

For many years soils engineers have been concerned with further understanding of the process of consolidation, for making more accurate settlement analysis of foundations. One of the assumptions used in Terzaghi's (1-D) theory was that all strains and flow occur in one direction only. In reality, however, very few cases such as consolidation in oedometer and consolidation of a thin layer with respect to a large area of uniform loading satisfy this assumption. Published field data given by Skempton and Bjerrum [29], on the rate of clay settlement indicate that the actual rates of settlement are generally faster than those predicted by the 1-D theory. This observation is particularly true for settlement of overconsolidated clays.

---

* Numbers in brackets refer to references given in the Bibliography.

The limitations of one-dimensional theory were clearly realized by engineers and an examination of the theory led to: (1) The Terzaghi-Rendulic [21] three-dimensional theory or "pseudo-three-dimensional" theory, Schiffman [26], and; (2) The three-dimensional (3-D) primary consolidation theory formulated by Biot [3]. Biot's theory couples the deformations and pore water pressures with the progress of consolidation, is more rational, and includes several factors that have been ignored in the previous theories. The governing equations for Biot's theory are more complex than the conventional theory and analytical solutions for practical problems are difficult to obtain. This difficulty is attributed first to the fact that soil in nature is nonhomogeneous, anisotropic, and nonlinear, and secondly, that geometric or boundary conditions can not be easily accommodated in closed-form solutions. However, with the increasing use of digital computers, several numerical methods have been developed and applied for incorporation of general consolidation theories. The two numerical methods that are most widely applied are the finite difference (FD) and finite element (FE) methods. The FD method has been applied in 1-D consolidation but its use in two-and three-dimensional problems is limited. The FE method has been proven to be more powerful for solutions of 1-D and 2-D problems, and two procedures have been recently proposed by Sandhu [22], Sandhu and Wilson [23], and by Christian and Boehmer [5]. From the two formulations, the one developed by Sandhu and Wilson is more general and has been used by a number of researchers. Most of the previous applications have been in homogeneous soils with 2-D consolidation under a strip footing.

Solutions for multi-layer systems have been obtained by 1-D FE formulation, FD methods and analytical methods. Applications of the FE method for practical problems involving 2-D consolidation of multi-layered systems have not yet been fully realized. It is the purpose of this thesis to analyze the various factors associated with 2-D consolidation of layered soils.

Numerical characteristics such as convergence and stability play an important part in the successful implementation of a numerical procedure. These factors have not been fully investigated for the FE procedure, Desai [9]. Numerical characteristics can be analyzed by two procedures, mathematical and quantitative or parametric. The former is usually possible for linear, homogeneous, isotropic systems with equal spatial and timewise subdivisions. Realistic problems involve nonlinear nonhomogeneous systems in which unequal mesh layouts are used. One of the aims of this study has been to arrive at guidelines for selection of optimum parameters for reliable answers.

Scope of Investigation

It is the intent of this thesis to encompass the following three topics:

1. Analyze practical problems of multi-layered soil systems. The relative magnitudes of permeability and Young's modulus and their effect on the process of consolidation was investigated using a three-layered system of clay-sand-clay under a strip footing.

2. Perform a quantitative study for convergence and accuracy.
3. Study the effects of strength and permeability anisotropy on the rate of consolidation for a homogeneous clay layer under plane strain.

Chapter Two

LITERATURE REVIEW

It is the intent of this chapter to present a review of publications most closely related to this thesis. Schiffman, et al [26], have given a good review and comparison of the Terzaghi 1-D, Terzaghi-Rendulic pseudo 3-D and Biot's theories.

Biot [3] in 1941 derived the complete three-dimensional consolidation theory for an ideal soil and the equations derived are based on Darcy's law for water flow through soil. The formulation provides coupling between the magnitude, progress of settlement and pore water pressures. Closed-form solutions using Biot's equations, for different loadings and geometry, have been obtained by a number of investigators. For uniformly loaded strip footing on a semi-infinite mass of soil, solutions have been obtained by Biot [3], Biot and Clingan [4], McNamee and Gibson [19], Schiffman, et al [27].

Cryer [7] in 1963 applied Biot's theory to the problem of a sphere subjected to hydrostatic pressure, and showed that an increase in excess pore pressure above the initial value occurs in the early stages of consolidation before actual pore water pressure dissipation occurs. The same phenomenon was also noted by Mandel [18] and it is known as the Mandel-Cryer effect. The Mandel-Cryer effect is not exhibited by the 1-D or pseudo 3-D theory and the results for the early stages of consolidation can be seriously in error. Davis and Poulos [8] have given a useful discussion of this topic. Cryer pointed out that for 1-D problems Biot's theory reduces to 1-D conventional theory. The mathematical consistency

for 1-D problems between the two theories was found by Sandhu [22].

Sandhu formulated a FE procedure based on Biot's theory of consolidation to obtain numerical solutions of displacement and pressure fields in two-dimensional laminar incompressible fluid flow through linearly elastic, isotropic saturated soil. The analysis requires the solution of a series of linear algebraic equilibrium and continuity equations expressed in terms of discrete values of displacement and pore pressure fields. Further details of the formulation are given in chapter three. Specializations to one- and two-dimensional problems have been proposed and used by various investigators. Desai and Johnson [11] developed a FE formulation based on the idealization of 1-D consolidation. A linear and a cubic approximating models were used and were compared for accuracy, stability, and computational effort. It was found that the linear model was more suitable for 1-D analysis and it was applied in the consolidation of a two- and three-layered cohesive soil system. The results were compared against experimental and closed-form solutions and the agreement was found to be good. The experimental observations were obtained from work done by Barden and Younan [2]. Hwang, et al [15] used the 2-D FE formulation and applied it to some plane strain problems. FE solutions were obtained for the problem of a uniform strip loaded half-plane and were compared with closed-form solutions obtained by Schiffman [26] and McNamee and Gibson [19]. The agreement between the solutions was good. Valliappan, et al [31], also used the foregoing formulation and solved plane strain problems previously solved by analytical methods by Gibson et al [14]. A two-layered soil system with

small variations in material properties was solved.

Yokoo et al [33] developed a FE formulation based on Biot's consolidation theory. The procedure used was similar to the one by Sandhu and Wilson with minor variations. The method was applied to one-dimensional and axisymmetric consolidation problems; anisotropy was considered in the axisymmetric case.

Abbott [1] in 1960 developed a FD method using the conventional 1-D equation. The method was applied in an actual field problem. The settlements computed by the method varied considerably from the recorded ones, particularly in the early stage of consolidation. Treatment of the interfaces between the layers can be the main difficulty in the FD method. The FD method was further applied to multi-layered soil systems by Murray [20]. He developed two computer programs for one- and two-dimensional (locally one-dimensional) consolidation. For his 2-D formulation the A and B parameters were used in computing the values of excess pore water pressures. A non-linear stress strain behavior was also considered in the program. This procedure is considered not to be general since one can obtain any form of results by varying A and B. Schiffman and Stein [28], using an analytical procedure, solved a multi-layer problem.

Chapter Three

FINITE ELEMENT THEORY

The finite element method has been found to be effective for approximate solutions of boundary value and initial boundary value problem. Details of the method have been published extensively, and a recent book by Desai and Abel [12] contains many applications of the method and a short bibliography of important contributions. In the following the formulation by Sandhu [22] is presented and is based on the description and notation given by Desai [9].

Governing Field Equations

The general three-dimensional theory formulated by Biot [3] is based on the following assumptions:

a. Small strains and small displacements.

b. The skeleton of solid particles is linearly elastic in terms of effective stress.

c. The soil is saturated with incompressible fluid.

d. Darcy's law is valid for fluid flow.

The following equations and boundary conditions must be satisfied in the process of consolidation, Figure 1.

1. Equilibrium Equations

$$\sigma'_{ij,j} + \delta_{ij}\, p_{,j} + \rho F_i = 0 \qquad (1)$$

where σ'_{ij} = components of effective stress tensor, p = pore water pressure, ρ = mass density of the soil, F_i = components of body force

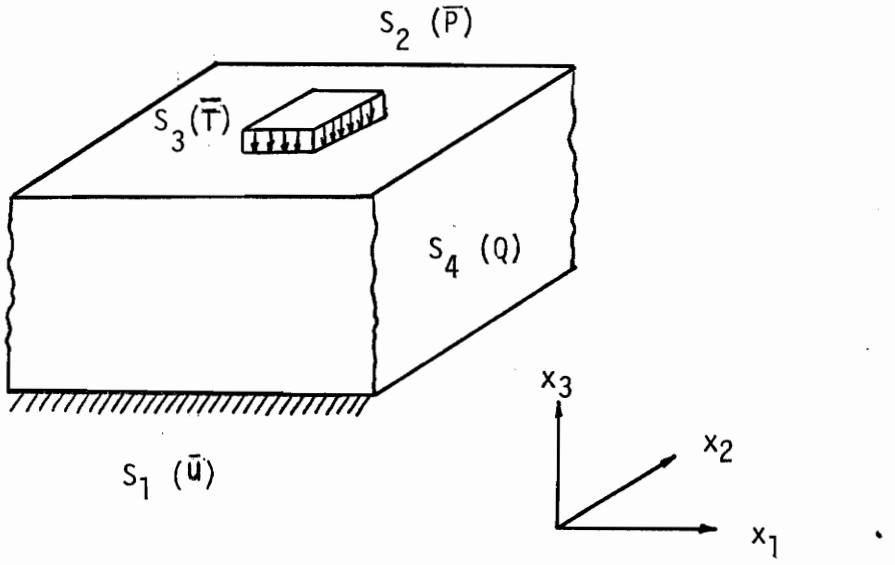

Figure 1. Schematic Diagram of Consolidation Problem and Boundary Conditions.

1, 2, 3 = primary nodes

4, 5, 6 = secondary nodes

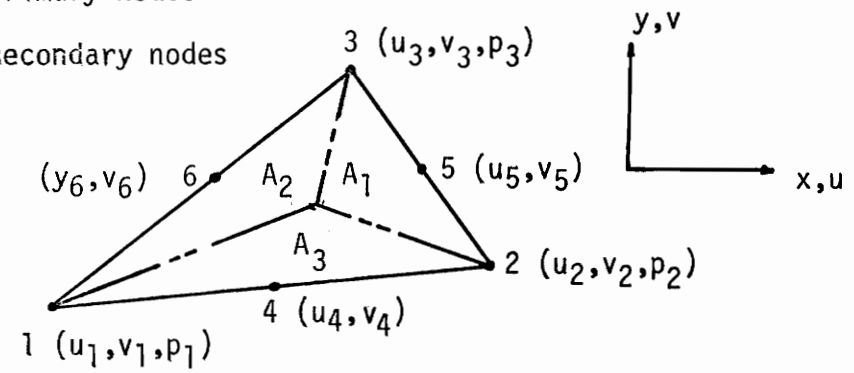

Figure 2. Triangular Element.

vector, δ_{ij} = Kronecker delta, and the comma in $p_{,j}$ denotes partial derivative.

2. Equations of Continuity

$$k_{ij}\ (p_{,j} + \rho_w F_j) + \dot{u}_{i,i} = 0 \qquad (2)$$

where k_{ij} = components of the permeability tensor, ρ_w = mass density of the fluid and u_i = components u, v, and w of the displacement vector in the three-coordinate directions x_1, x_2, and x_3, Figure 1.

3. Boundary Conditions

a. Applied displacements, $\bar{u}_i$, on a part of the boundary S_1

$$u_i = \bar{u}_i \qquad (3a)$$

b. Applied pore water pressure, $\bar{p}$, on a part of the boundary S_2

$$p = \bar{p} \qquad (3b)$$

c. Applied traction or surface loading, $\bar{T}_i$, on a part of the boundary S_3

$$\bar{T}_i = (\sigma_{ij} + \delta_{ij}p)n_j \qquad (3c)$$

where n_j is the unit normal vector.

d. Applied fluid flow, $\bar{Q}$, on a part of the boundary S_4

$$\bar{Q} = q_i n_i \qquad (3d)$$

4. Stress-strain Relationship

$$\sigma'_{ij} = C_{ijkl} e_{kl} \qquad (4a)$$

where C_{ijkl} = components of the elastic moduli of the soil skeleton in terms of effective stress, e_{kl} = components of strain tensor given by

$$e_{ij} = 1/2\ (u_{i,j} + u_{j,i}) \tag{4b}$$

5. Generalized Darcy's Law

$$q_i = k_{ij}\ (p_{,j} + \rho_w F_j) \tag{5}$$

where q_i = components of fluid flux vector.

The variational principle used for deriving the FE equations is given by

$$A\ (u_i, p) = \int_V 1/2\ \sigma'_{ij} * u_{ij} - \rho F_i * u_i + p * u_{i,i} - 1/2\ g * q_i * (p_{,i} + \rho_w F_i)\ dV - \int_{S_3} (\overline{T}_i * u_i)\ dS + \int_{S_4} (g * \overline{Q} * p)\ dS \tag{6}$$

Here * denotes convolution and is defined as

$$f_1 * f_2 = \int_0^t f_1\ (x_i, \tau)\ f_2\ (x_i, t-\tau)\ d\tau \tag{7}$$

and g = 1.

Approximation for Displacement and Pore Water Pressures

In the FE procedure, the displacements and pore water pressures are approximated by using interpolation functions, Desai and Abel [12], Desai [9], as

$$\begin{Bmatrix} u \\ v \\ w \\ p \end{Bmatrix} = \begin{bmatrix} [N_u] & 0 & 0 & 0 \\ 0 & [N_u] & 0 & 0 \\ 0 & 0 & [N_u] & 0 \\ 0 & 0 & 0 & [N_p] \end{bmatrix} \begin{Bmatrix} \{u(t)\} \\ \{v(t)\} \\ \{w(t)\} \\ \{p_n(t)\} \end{Bmatrix} \tag{8}$$

or $= [N] \begin{Bmatrix} \{q(t)\} \\ \{p(t)\} \end{Bmatrix}$

where $\{u(t)\}^T = [u_1, u_2, \ldots u_n]$

$\{v(t)\}^T = [v_1, v_2, \ldots v_n]$

$\{w(t)\}^T = [w_1, w_2, \ldots w_n]$

$\{p_n(t)\}^T = [p_1, p_2, \ldots p_n]$

$[N_u] = [N_{u1}, N_{u2}, \ldots N_{un}]$

$[N_p] = [N_{p1}, N_{p2}, \ldots N_{pn}]$

N_{ui} and N_{pi} = interpolation functions

N = degrees of freedom at a node

$\{u(t)\}$ = vector of nodal displacements in the x-direction, etc.

$\{p_n(t)\}$ = vector of nodal pore water pressures, and

$\{q(t)\}^T = [\{u(t)\}^T \{v(t)\}^T \{w(t)\}^T]$

The notation for matrices and vectors used herein is:

Rectangular Matrix: $[A]$

Column Matrix (vector) : $\{A\}$

Row Matrix (vector): $\{A\}^T$

where the superscript T indicates the transpose.

Substitution of Equation 8 and its proper derivatives in Equation 6 and vanishing of the variation of the resulting functional yields the element matrix equations. Assembly of element equations then yields the global relation as

$$[K] \{r_u(t)\} + [K^*] \{r_p(t)\} = -\{M_1\} + \{M_2\} + \{P_1\} \quad (9)$$

and $[K^*]^T \{r_u(t)\} - g * [\overline{K}] \{r_p(t)\} = g^* \{M_3\} - g * \{P_2\}$ (10)

Equation 9 is the equilibrium equation in which

$[K] \{r_u(t)\}$ = nodal force vector due to the straining of soil skeleton,

$[K^*] \{r_p(t)\}$ = nodal force vector resulting from the pore pressure,

$\{M_1\}$ = load vector due to initial stresses existing in the soil before the application of external load,

$\{M_2\}$ = load vector due to the body forces,

$\{P_1\}$ = specified boundary traction vector (Locally applied loads are included in $\{P_1\}$.),

and Equation 10 represents the continuity of flow in which:

$[K^*]^T \{r_u(t)\}$ = the volumetric strain of soil skeleton,

$g^*[E]\{r_p(t)\}$ = the fluid inflow due to pore pressure,

$g^* \{M_3\}$ = the fluid flow due to fluid gravity force,

$g^* \{P_2\}$ = the fluid flow due to specified boundary flow (Local drainages applied at nodes are added to $\{P_2\}$.)

and where $\{r_u(t)\}$ and $\{r_p(t)\}$ = vectors of global nodal displacements and pore water pressures, respectively. Further details of the derivations are given in references 9, 15, 22, 23, 24, 32, and 33.

Presented here are statements, in matrix form, for the equations involved [9]:

$$[K] = \sum_{i=1}^{m} \int_V [B_e]^T [C][B_e] \, dV \qquad (10a)$$

$$[K^*] = \sum_{i=1}^{m} \int_V [B_\Delta]^T \{N_p\} \, dV \qquad (10b)$$

$$[\bar{K}] = \sum_{i=1}^{m} \int_{V} [B_q]^T [r] [B_q] \, dV \qquad (10c)$$

$$\{M_1\} = \sum_{i=1}^{m} \int_{V} [B_e]^T \{\sigma_0\} \, dV \qquad (10d)$$

$$\{M_2\} = \sum_{i=1}^{m} \int_{V} [N_u] \{\rho F\} \, dV \qquad (10e)$$

$$\{M_3\} = \sum_{i=1}^{m} \int_{V} [B_q]^T [R] \{\rho_w F\} \, dV \qquad (10f)$$

$$\{P_1\} = \sum_{i=1}^{m} \int_{S_3} [N_u]^T [N_u] \{\bar{T}\} \, dS \qquad (10g)$$

$$\{P_2\} = \sum_{i=1}^{m} \int_{S_4} [N_p]^T [N_p] \{\bar{Q}\} \, dS \qquad (10h)$$

where various matrices and vectors are given by

strain vector $\{\varepsilon\} = [B_e] \{q\}$ (11a)

effective stress vector $\{\sigma'\} = [C] [B_e] \{q\} + \{\sigma_0\}$ (11b)

where $[B_e]$ = transformation matrix obtained by appropriate differentiation of the displacement field,

volumetric strain vector $\{\varepsilon_v\} = [B_\Delta] \{q\}$ (11c)

gradient of pore pressure vector

$$\frac{\partial p}{\partial x_i} = [B_q] \{p_n\} \qquad (11d)$$

$\{\sigma_0\}$ = vector of initial stresses and $[C]$ = stress-strain matrix, $[R]$ = matrix coefficients of permeability, and m = number of elements.

Time Integration

Equation 9 and 10 represent FE discretization in space in which

Equations 10 are matrix differential equations in time. Solutions for $\{r_u\}$ and $\{r_p\}$ now require integration of these equations with respect to time.

The terms with convolution product in Equation 10 can be written by using the following general relation:

$$g * F_1(t) = \int_0^t F(\tau) \cdot g\,(t-\tau) = \int_0^t F(\tau)\, d\tau \qquad (12a)$$

because $g(t-\tau) = 1$. If we choose discrete time interval of Δt then,

$$\int_t^{t+\Delta t} F(\tau)\, d\tau = \alpha\Delta t\, F(t + \Delta t) + (1-\alpha)\ \Delta t + F(t) \qquad (12b)$$

The Crank-Nicholson type of time integration introduced in Equation 10 gives the following equations:

$$[K]\,\{r_u\}_{t+\Delta t} + [K^*]\,\{r_p\}_{t+\Delta t} = -\{M_1\}_{t+\Delta t} + \{M_2\}_{t+\Delta t} + \{P_1\}_{t+\Delta t} \qquad (13a)$$

$$[K^*]^T\,\{r_u\}_{t+\Delta t} - \frac{\Delta t}{2}\,[\overline{K}]\,\{r_p\}_{t+\Delta t} = [K^*]^T\{r_u\}_t + \frac{\Delta t}{2} + [\overline{K}]\{r_p\}_t + \frac{\Delta t}{2}\,[\{M_3\}_t + \{M_3\}_{t+\Delta t}] - \frac{\Delta t}{2}\,[\{P_2\}_t + \{P_2\}_{t+\Delta t}] \qquad (13b)$$

This may be written in the form

$$\left[\begin{array}{c|c} [K] & [K^*] \\ \hline [K^*] & -\frac{\Delta t}{2}[\overline{K}] \end{array}\right] \left\{\begin{matrix}\{r_u\} \\ \{r_p\}\end{matrix}\right\}_{t+\Delta t} = \left\{\begin{matrix}\{R_u\} \\ \{R_p\}\end{matrix}\right\} = \{R\} \qquad (14)$$

where $\{R\}$ = vector of nodal forcing parameters due to loads and pore water pressures and its components are known. These equations are solved at $t + \Delta t$ after boundary conditions are introduced, and the

solution is propagated in time. The first solution is obtained at $t = \Delta t$ since $\{r\}^T = [\{r_u\}^T\{r_p\}^T]$ are known at $t = 0$.

For all the solutions obtained in this thesis, the total time was divided into various time periods and a variable Δt was used for each time period. Effect of magnitudes of Δt on the solution is discussed in Chapter 4. Triangular elements, Figure 2[23], were used for the formulation with quadratic variation for displacements and linear variation for pore water pressure given by

$$\left.\begin{aligned} u &= N_i U_i + N_j U_j \\ v &= N_i V_i + N_j V_j \end{aligned}\right\} \qquad \begin{aligned} N_i &= L_i(2L_i - 1) \\ N_j &= 4L_jL_k \end{aligned} \qquad (15)$$

$$i = 1, 2, 3$$

$$j = 1, 2, 3$$

$$k = 1, 2, 3$$

$$j \neq k, \quad i \neq j$$

$$p = N_m P_m \text{ and } N_m = L_i$$

where $L_i = A_i/A$ and A = area, Figure 2.

Triangular elements give satisfactory answers for many problems. However, they have two disadvantages:

a. Greater number of nodal points and elements are required which means more computer storage and time are required and,

b. They can yield skewness in the solutions and may require use of twice as many elements to obtain symmetry.

Chapter Four

ANALYSIS OF NUMERICAL PROPERTIES AND COMPARISONS

In order to examine the range of applicability of the formulation and code, a parametric study was performed for one- and two-dimensional problems. For the 1-D analysis the accuracy of the program was checked with closed-form solutions and convergence plots of pore water pressures were plotted for different times. For the 2-D analysis behavior of solution with mesh refinement was evaluated. Other factors examined were the effect of the relative distance to the boundaries, size of time increment, boundary conditions and Poisson's ratio.

One-Dimensional Consolidation

The cohesive soil mass was discretized into a number of sets of finite element meshes with 21, 33 and 63 nodes respectively, Figure 3. The material properties and boundary conditions are also shown in Figure 3. Three plots of error in pore water pressure (in percent) versus the number of nodes for T = 0.17, 0.336, and 0.42 are shown in Figures 4-6, respectively. The percent error was evaluated as the difference between Terzaghi and the FE solution, p*-p, where, Taylor [30],

$$p^* = \sum_{m=0}^{m=\alpha} \frac{2p_o}{M} \left(\sin \frac{Mz}{H}\right) e^{-M^2 T} \qquad (15)$$

in which, $M = 1/2\ \pi\ (2m + 1)$,

m = a dummy variable taking on values 1, 2, 3,...,

T = dimensionless time factor = $\frac{c_v t}{H^2}$,

p_o= initial pore water pressure,

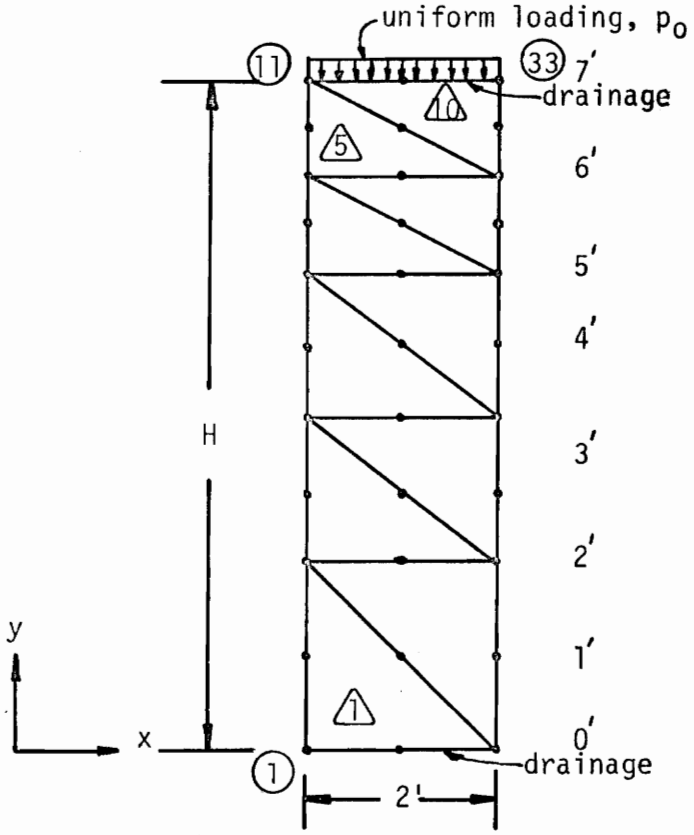

Mesh No. 2

Mesh No.	No. of Nodes
1	21
2	33
3	63

LEGEND

△ Element

○ Nodal Point

Material Properties

$E = 6000$ psf

$\nu = 0.4$

$k = 4 \times 10^{-6}$ ft/day

$\gamma_w = 62.5$ pcf

Figure 3. One-Dimensional Problem and FE Mesh Representation.

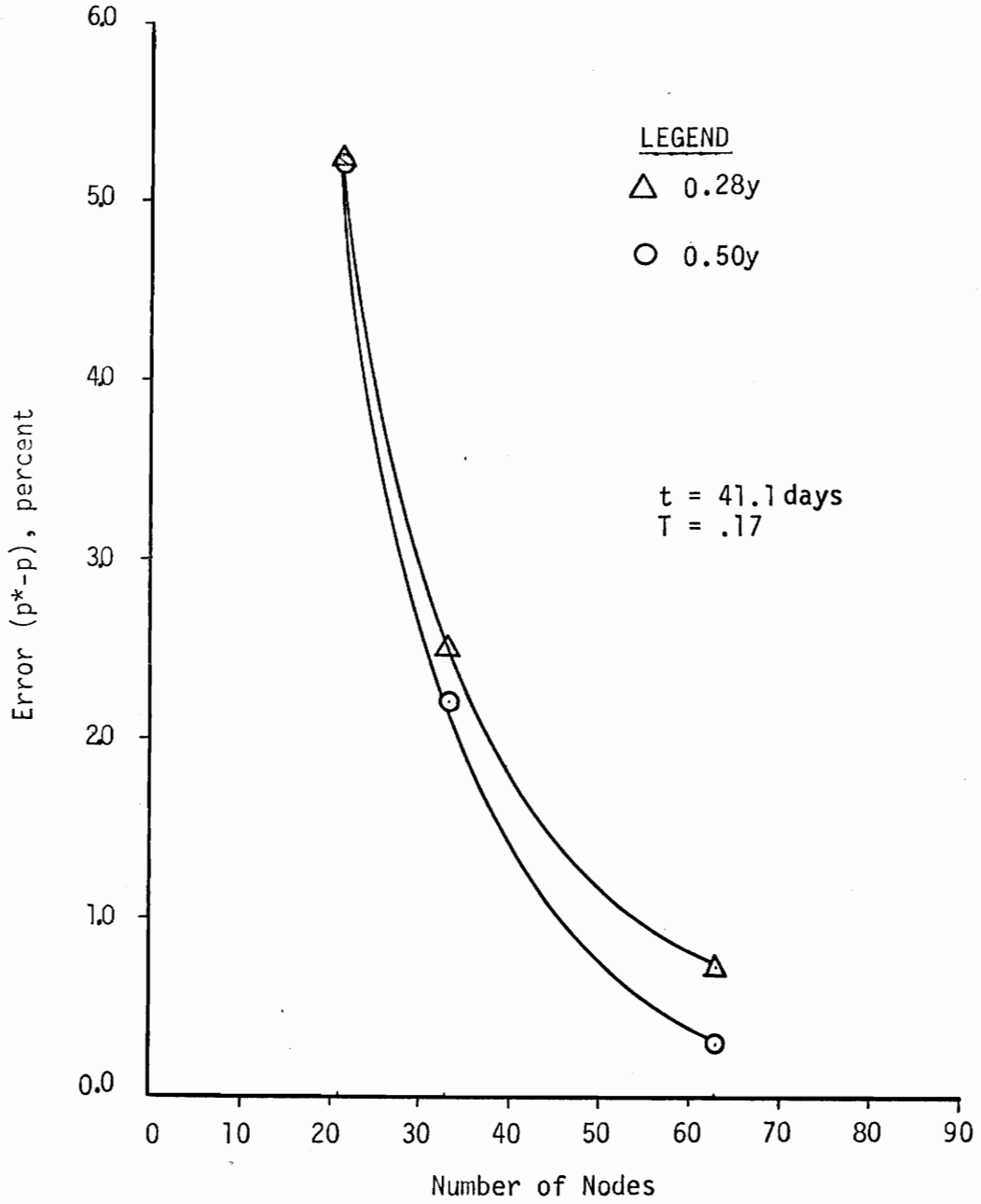

Figure 4. Convergence of Pore Water Pressures for 1-D Consolidation at T = 0.17.

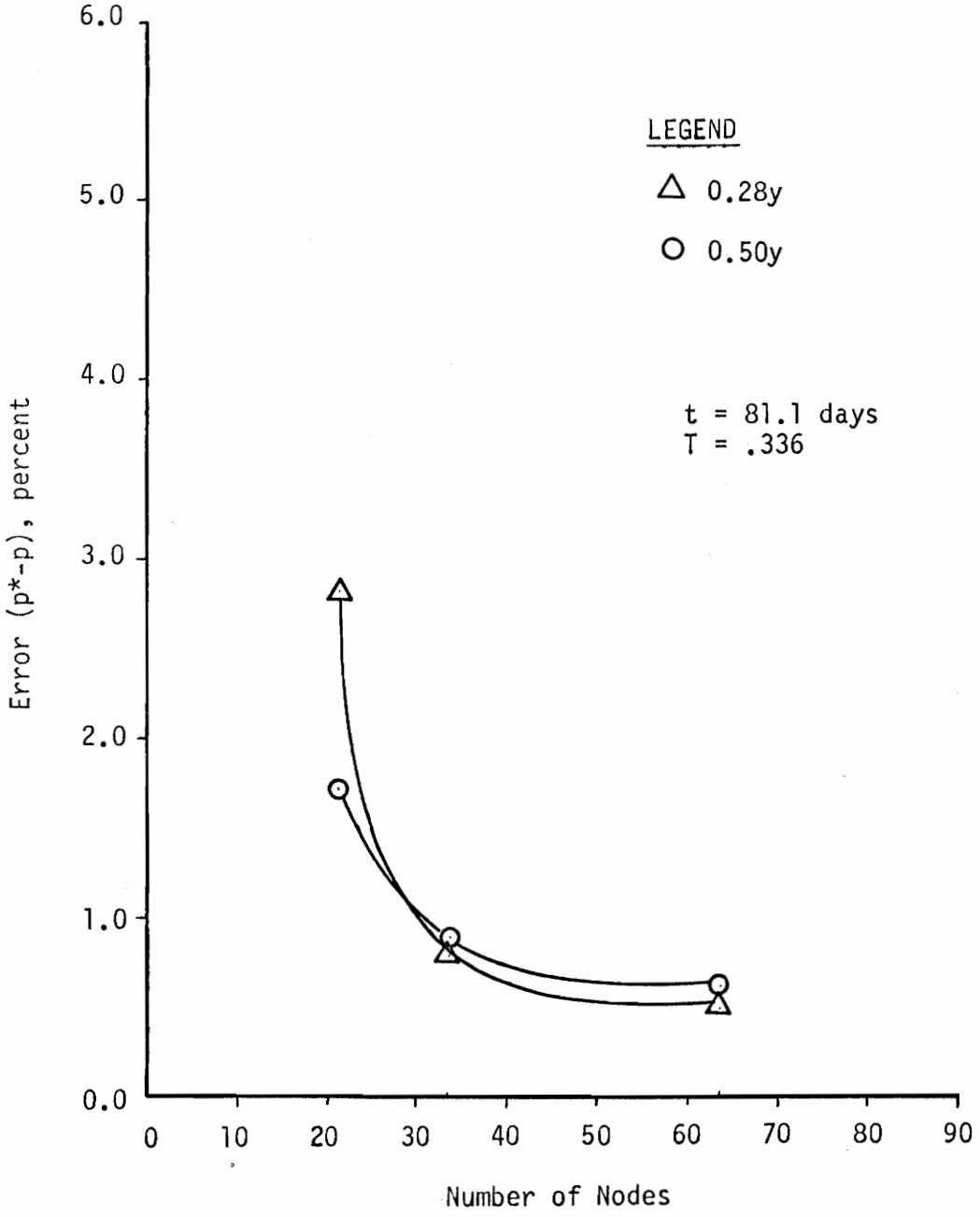

Figure 5. Convergence of Pore Water Pressures for 1-D Consolidation at T = 0.336.

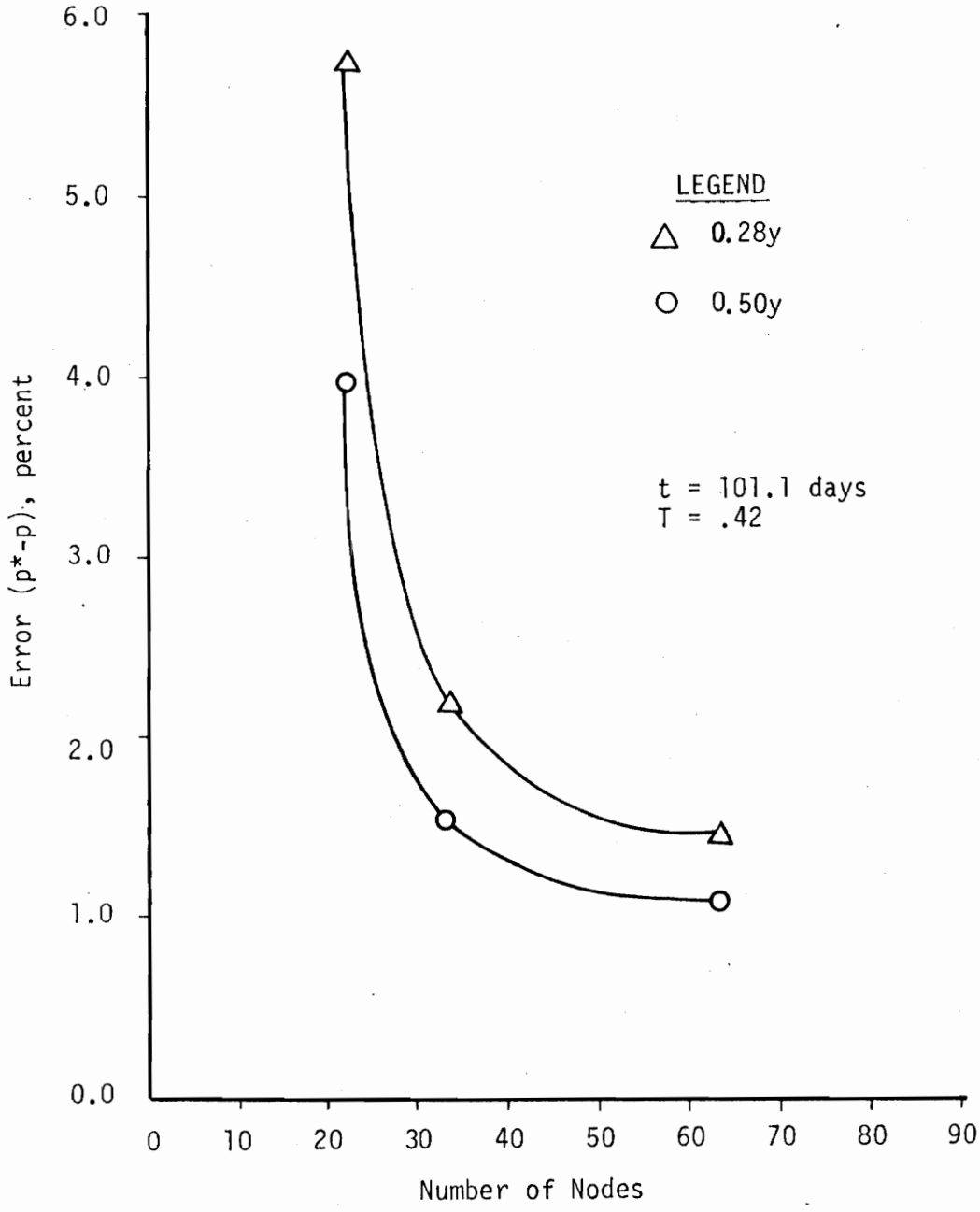

Figure 6. Convergence of Pore Water Pressures for 1-D Consolidation at T = 0.42,

p = computed pore water pressure at time t,

c_v = coefficient of consolidation for 1-D case,

t = real time of consolidation,

H = drainage path,

$c_v = \frac{k}{\gamma_w m_v}$,

γ_w = unit weight of water,

m_v = the coefficient of volume compressibility.

For all three time factors, Figures 4, 5 and 6, the accuracy of the FE solution improves with mesh refinement and it converges faster at the center (0.5y) than it does in the top regions of the soil mass, (0.28y). The distance y is taken from the surface of the soil mass.

Figure 7 shows comparisons for pore water distributions obtained by using Terzaghi theory for T = 0.087, 0.17, 0.25, and 0.42 and those from the FE method with 33 nodes. It is observed that both solutions are in close agreement. A similar study for 1-D consolidation done by Desai and Johnson [10] showed similar comparisons.

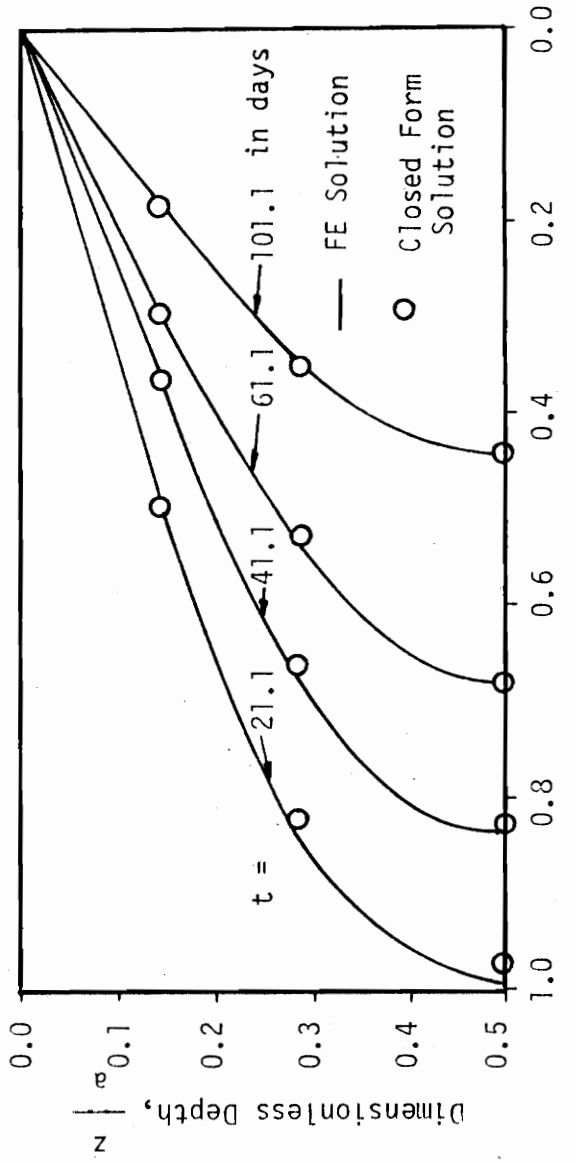

Figure 7. Distribution of Pore Water Pressure at Various Time Factors.

Two-Dimensional Consolidation

In order to study the numerical properties of the FE procedure in 2-D consolidation problems, the soil mass was discretized into a number of sets of FE meshes, Figure 8, with 25, 81 and 187 nodes. Pore water pressures p/p_0 versus a dimensionless factor λ are shown for different T and for three nodes within the mesh, Figures 9-12. The factor λ is defined as

$$\lambda = \frac{c_v \Delta\bar{t}}{\Delta\bar{x}^2+\Delta\bar{y}^2}, \tag{16}$$

in which $\Delta\bar{x} = \frac{\Sigma\Delta x_i}{M}$, (16a)

$\Delta\bar{y} = \frac{\Sigma\Delta y_i}{M}$, (16b)

$\Delta\bar{t} = \frac{\Sigma\Delta t}{n}$ (16c)

and n = number of different time increments used in the consolidation process,

t = real time of consolidation,

c_v = coefficient of consolidation,

M = number of elements,

$\Delta\bar{x}$, $\Delta\bar{y}$, $\Delta\bar{t}$ = mean values of spatial and timewise meshes.

The distance y shown in Figures 9-12 is taken from the surface of the discretized soil mass. It is observed that the solution does not show consistent behavior, particularly, at early time levels, $T = 2.5 \times 10^{-3}$, and $T = 4.5 \times 10^{-3}$ shown in Figures 9 and 10 respectively. At higher

levels, however, the solution behavior becomes consistent, as is shown in Figures 11 and 12. From the observations made above and other points of the solution it seems that a value of λ below 5.0×10^{-3} can yield reliable answers for two-dimensional analysis.

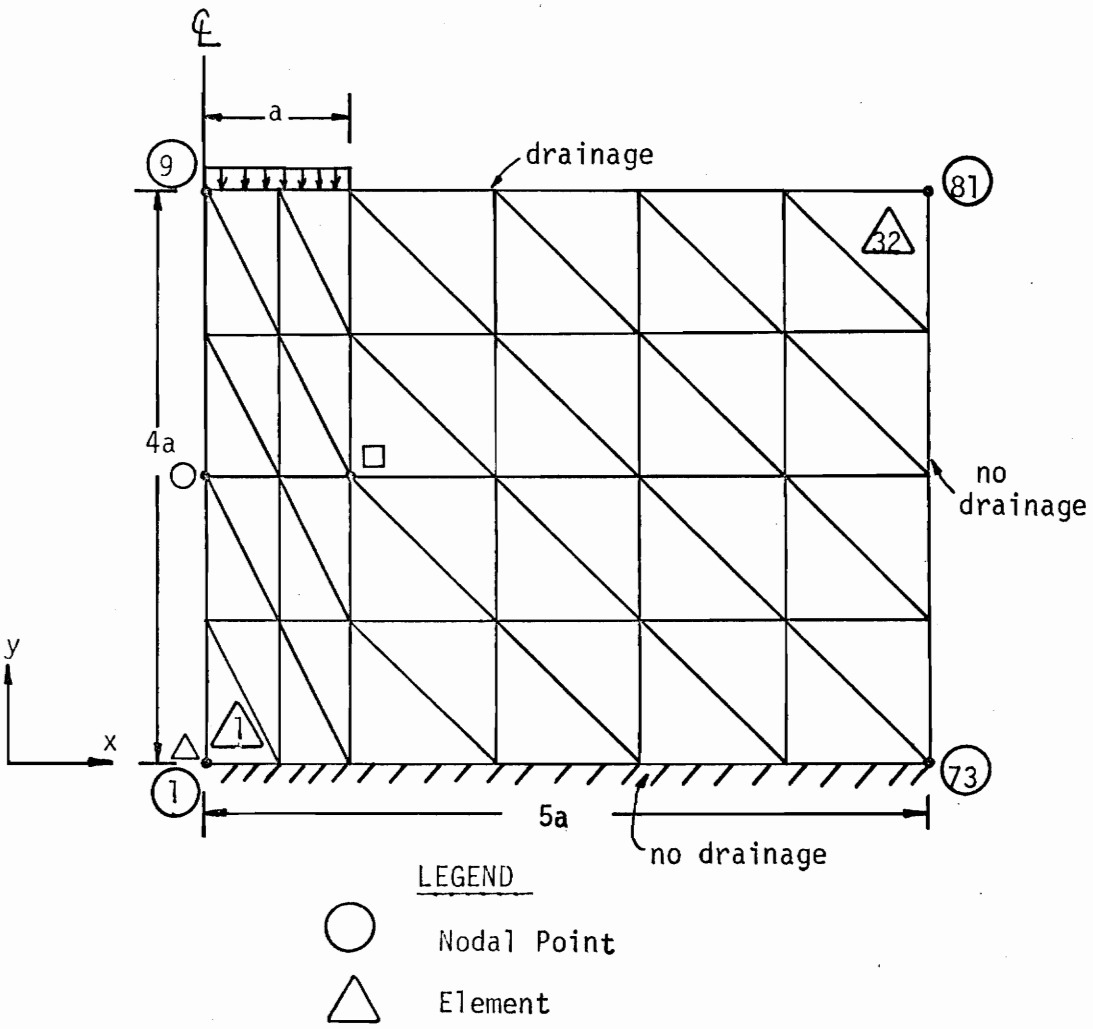

Mesh No.	No. of Nodes
1	25
2	81
3	187

$E = 85{,}000$ psf
$\nu = .3$
$k = 3.0 \times 10^{-5}$ ft/day
$\gamma = 51.0$ pcf

Figure 8. Finite Element Mesh used for Two-Dimensional Analysis.

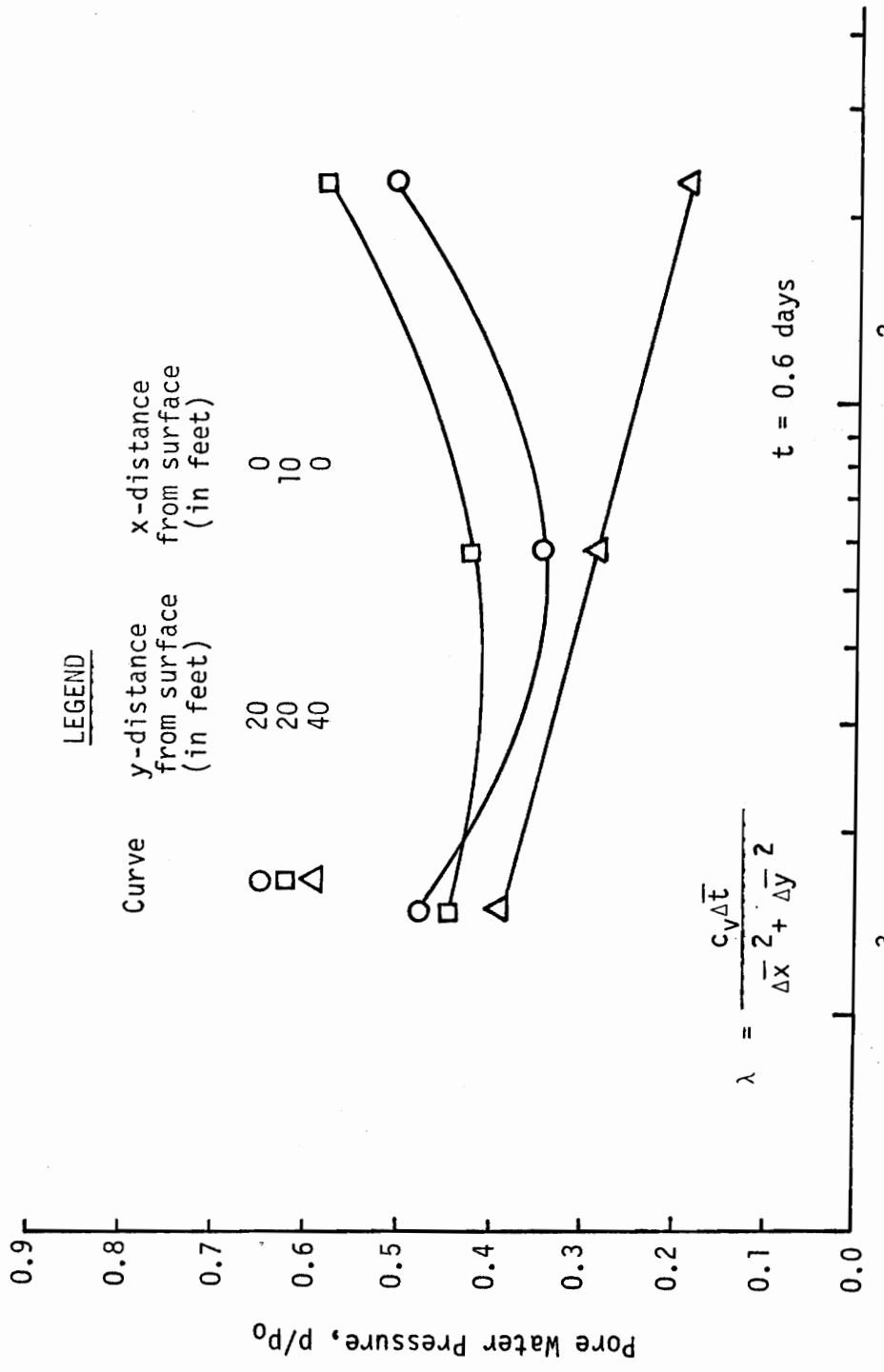

Figure 9. Pore Water Pressure at Various Nodal Points vs. λ, T = 2.5×10^{-3}.

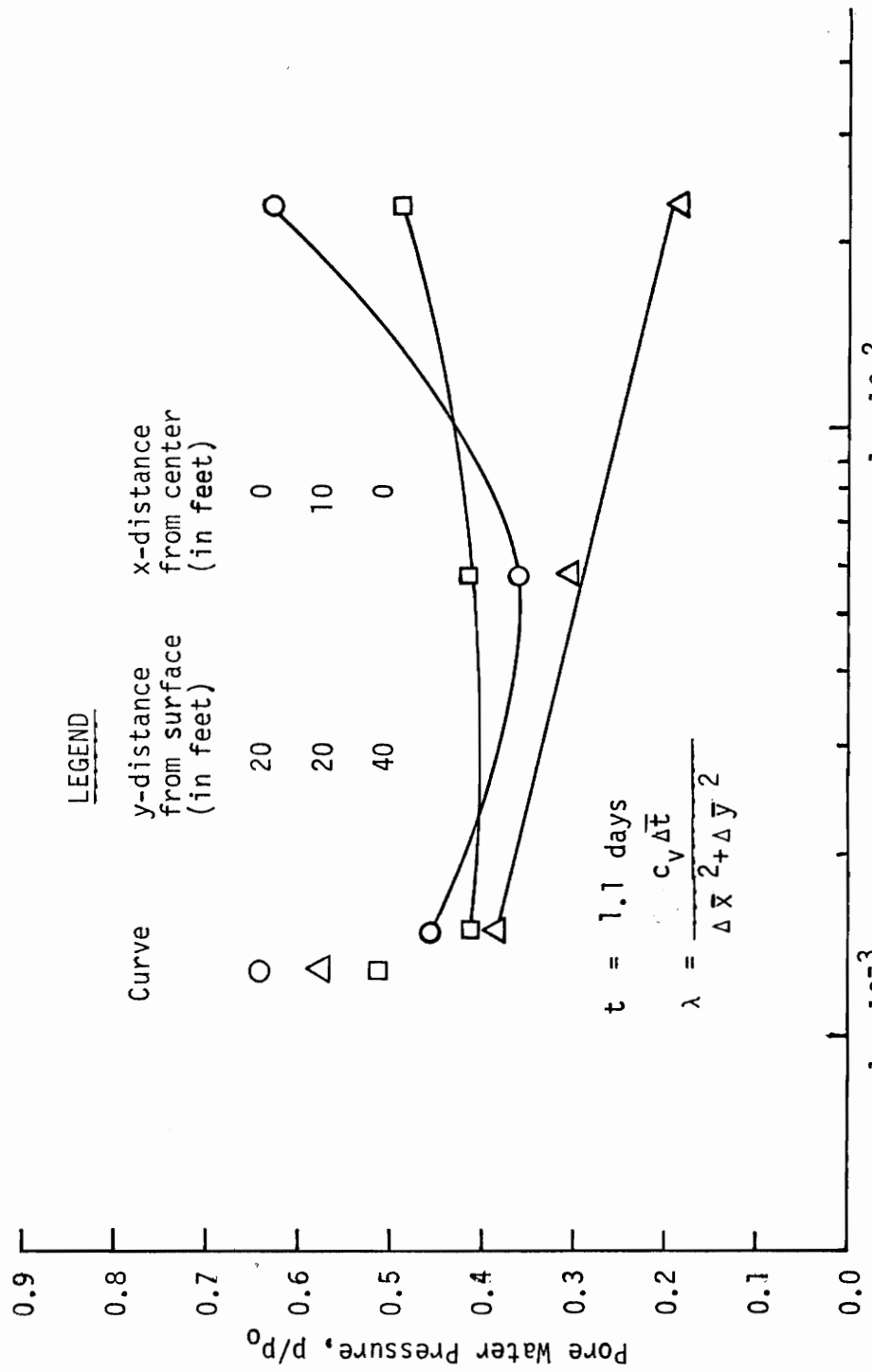

Figure 10. Pore Water Pressure at Various Nodal Points vs. λ , T = 4.5 x 10^{-3}

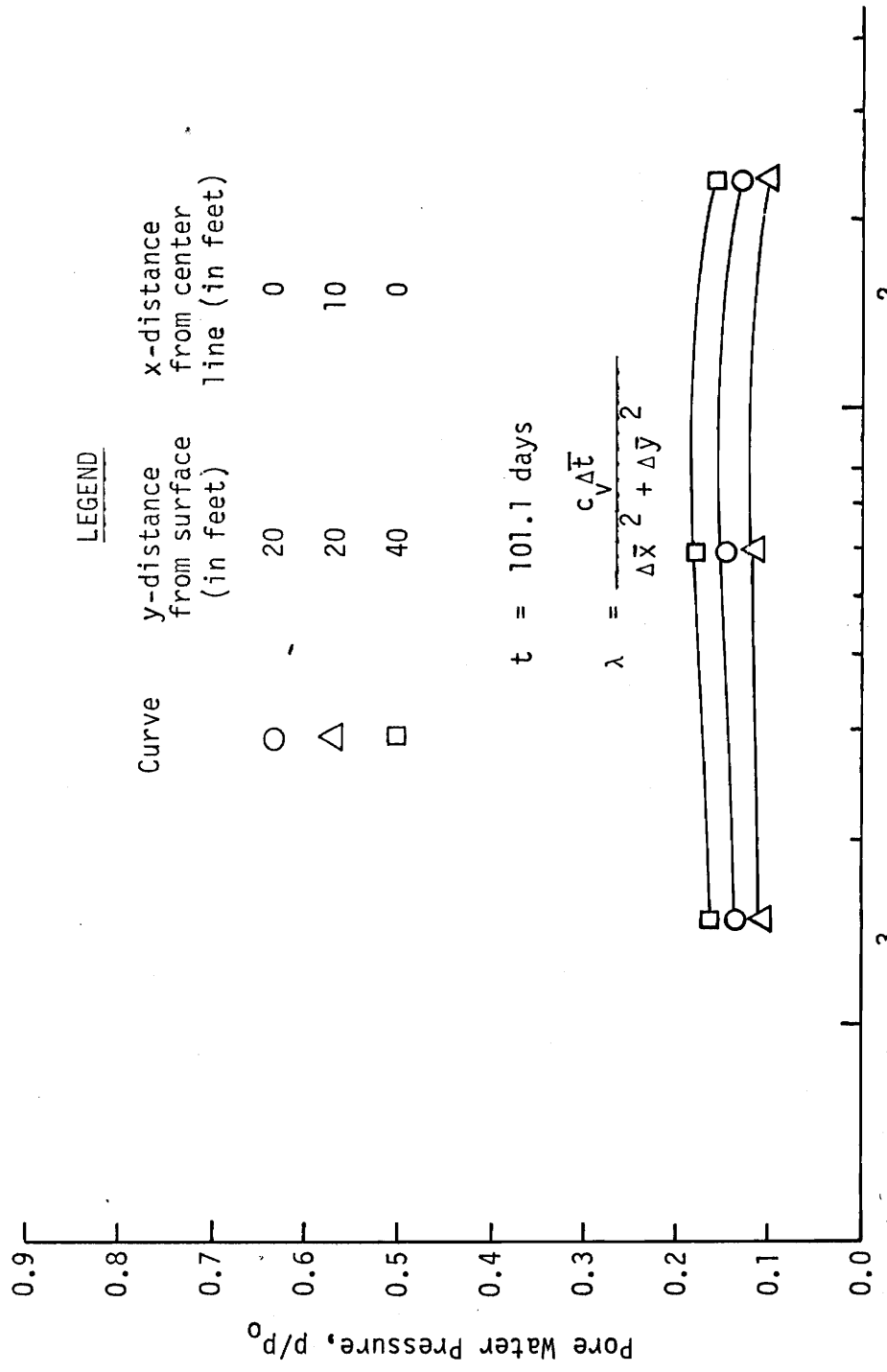

Figure 11. Pore Water Pressure at Various Nodal Points vs. λ. T = 0.42.

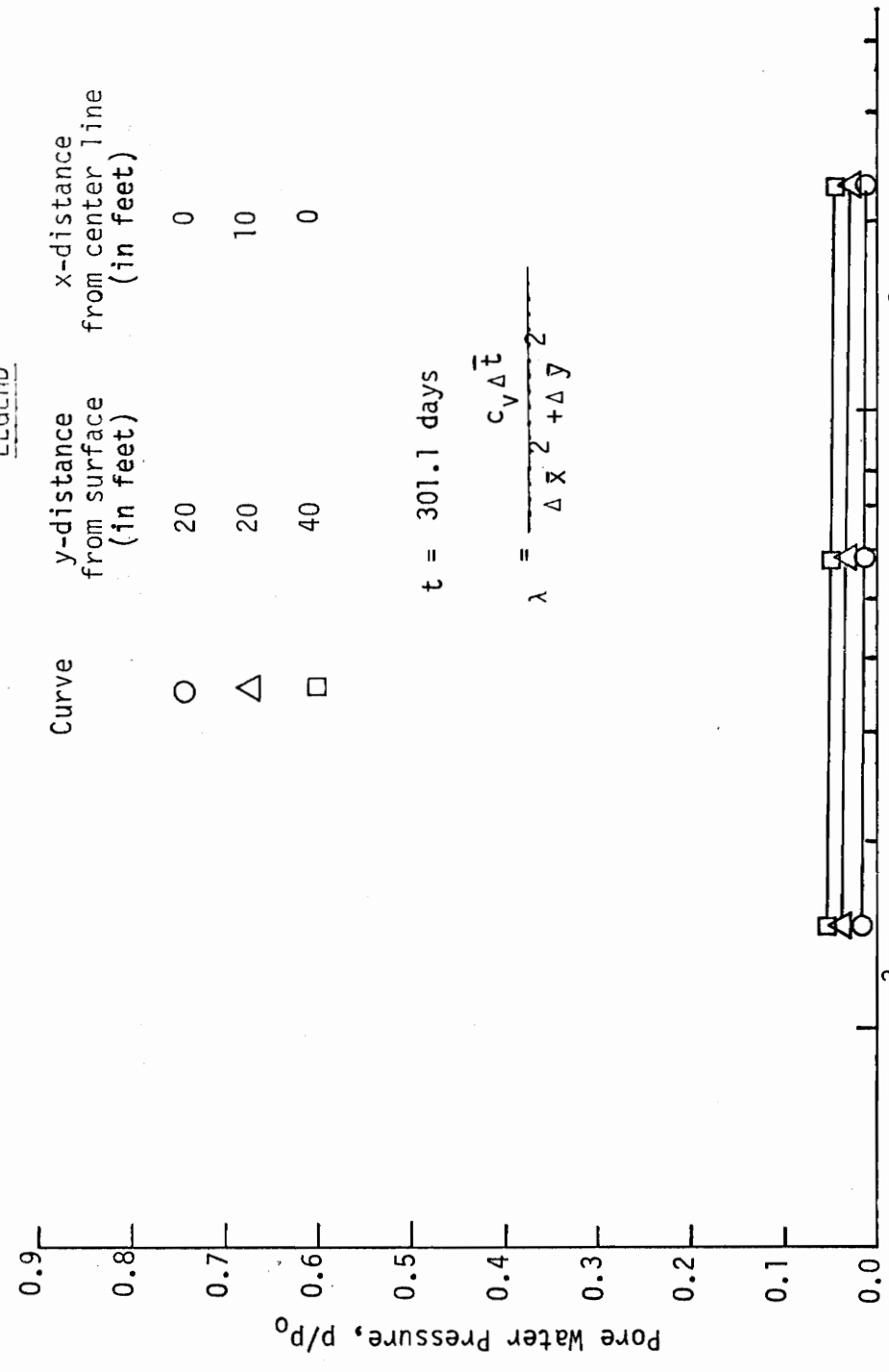

Figure 12. Pore Water Pressure at Various Nodal Points vs. λ , T = 1.25.

Effect of Poisson's Ratio

Figure 13 shows the effect of Poisson's ratio, ν, on the rate of consolidation settlement for the surface node at the center line. Geometry of the problem considered is shown in Figure 13 with the vertical boundary, H, at a distance 4a, where a is the width of the strip load, and the horizontal boundary at a distance of 32a from the center of the loaded area.

The coefficient of volume compressibility m_v is kept constant as it is assumed in the 1-D consolidation theory. The constraint modulus D is also assumed constant and was evaluated as follows:

$$D = \frac{1}{m_v} \tag{17}$$

Varying ν with constant D means that the Young's modulus E must change since

$$D = \frac{E(1-\nu)}{(1+\nu)(1-2\nu)} \tag{18}$$

and the time factor T is given by

$$T = \frac{c_v t}{H^2} \tag{19}$$

where

$$c_v = \frac{k}{\gamma_w} \frac{1}{m_v} \tag{20}$$

The different values of E used for the analysis are shown in Figure 13 where it can be observed that the higher the Poisson's ratio the higher the rate of consolidation settlement.

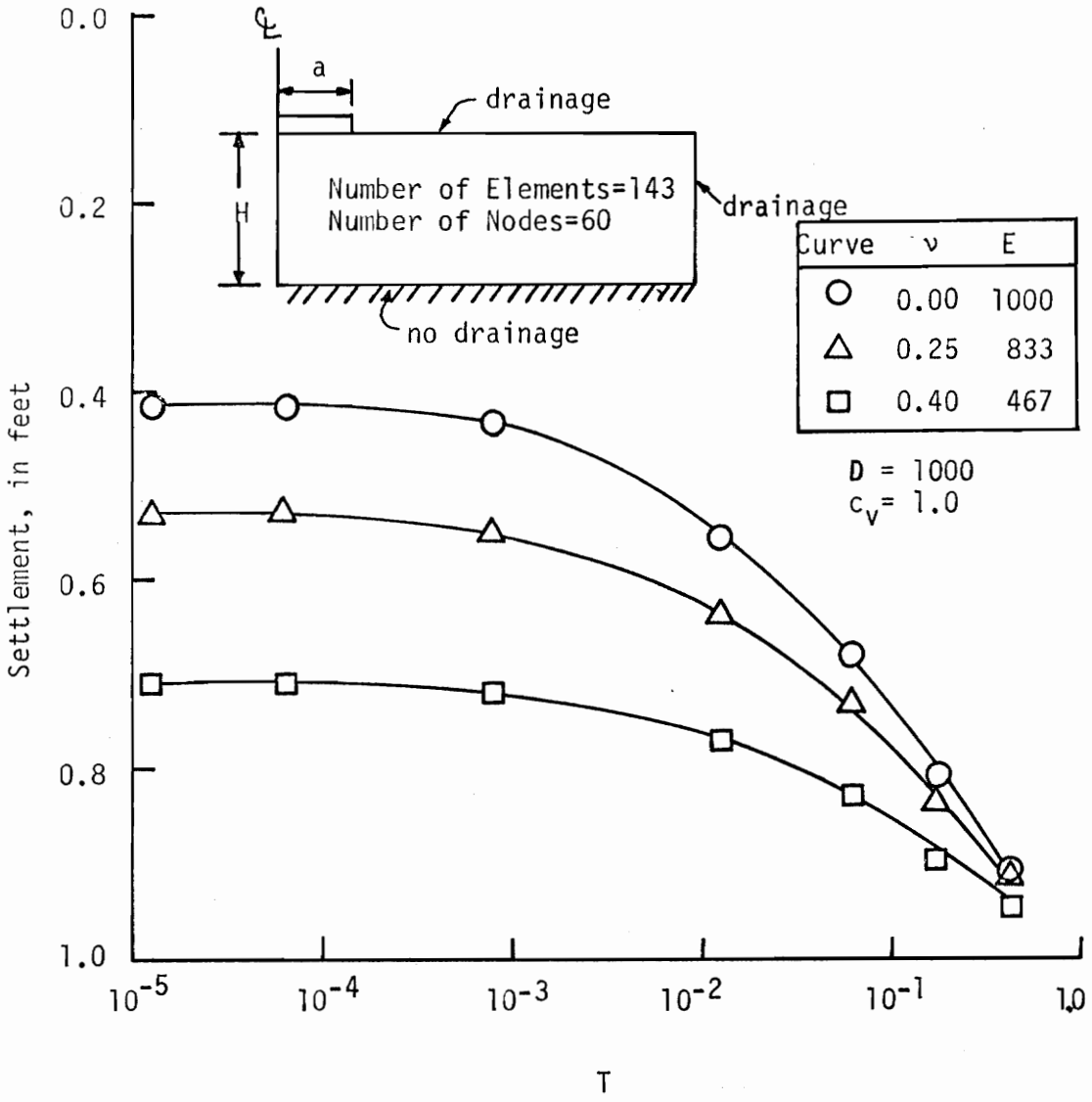

Figure 13. Consolidation Settlement at Top Node of the Center Line for Various ν and Constant D.

Effect of the Relative Distance to the Boundaries

Figure 14 shows plots for pore water pressure dissipation for a node located at the center line and at a depth a.

Two of the curves show results for the effect of changing the distance to the vertical boundary and one curve for the horizontal boundary in comparison with closed-form [26] and FE solutions [5]. The geometry of the problem and all material parameters used for the analysis are also given in Figure 14.

From the results it can be observed that changing the relative distance to the boundaries in the FE mesh can have a significant effect on the solution. The Mandel-Cryer effect is observed in all the solutions in Figure 14 where at early times of the consolidation process there is an increase of pore water pressures above the initial value, before actual pore water pressure dissipation occurs.

The Mandel-Cryer effect can be explained as follows. A short time Δt after loading the surface elements will have substantially drained. This drainage will increase the total and effective stresses with development of strains in these elements. In the time Δt, however, an interior element within the mesh has not started to drain and develop strains and effective stress increments. In order for the surface and interior elements to be compatible in strain, part of the total stress increment developed in the surface element will be transferred to the interior element. This will cause an increase in the total stresses applied to the interior elements. Therefore in the early stages of consolidation the total stress components will increase over the initial value.

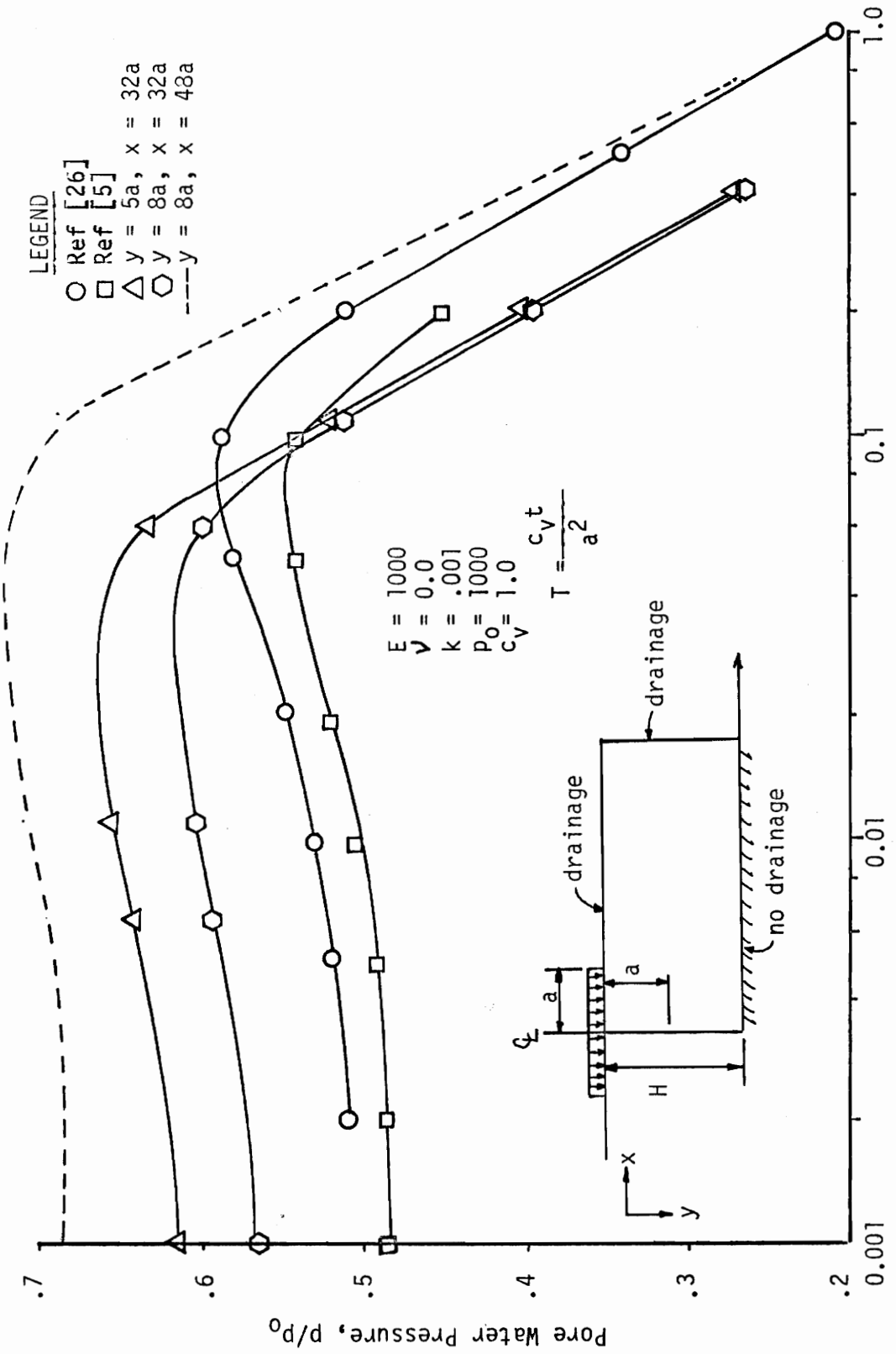

Figure 14. Pore Water Pressure versus Time at Center Line and Depth a.

Effect of Time Increment

As it was mentioned in Chapter Three under Time Integration, the total time for consolidation was divided into various time periods with a different value of time increment Δt to improve the efficiency of the solution and obtain more readings, particularly in the early stages of the consolidation process. To check the effect of changing Δt on the solution, the same problem shown in Figure 14 was analyzed by keeping Δt constant. It can be observed from Figure 15 that the solution for both constant and variable Δt seem to yield similar results. The pore water pressure distribution is plotted for the nodal point along the center line and distance a from the top.

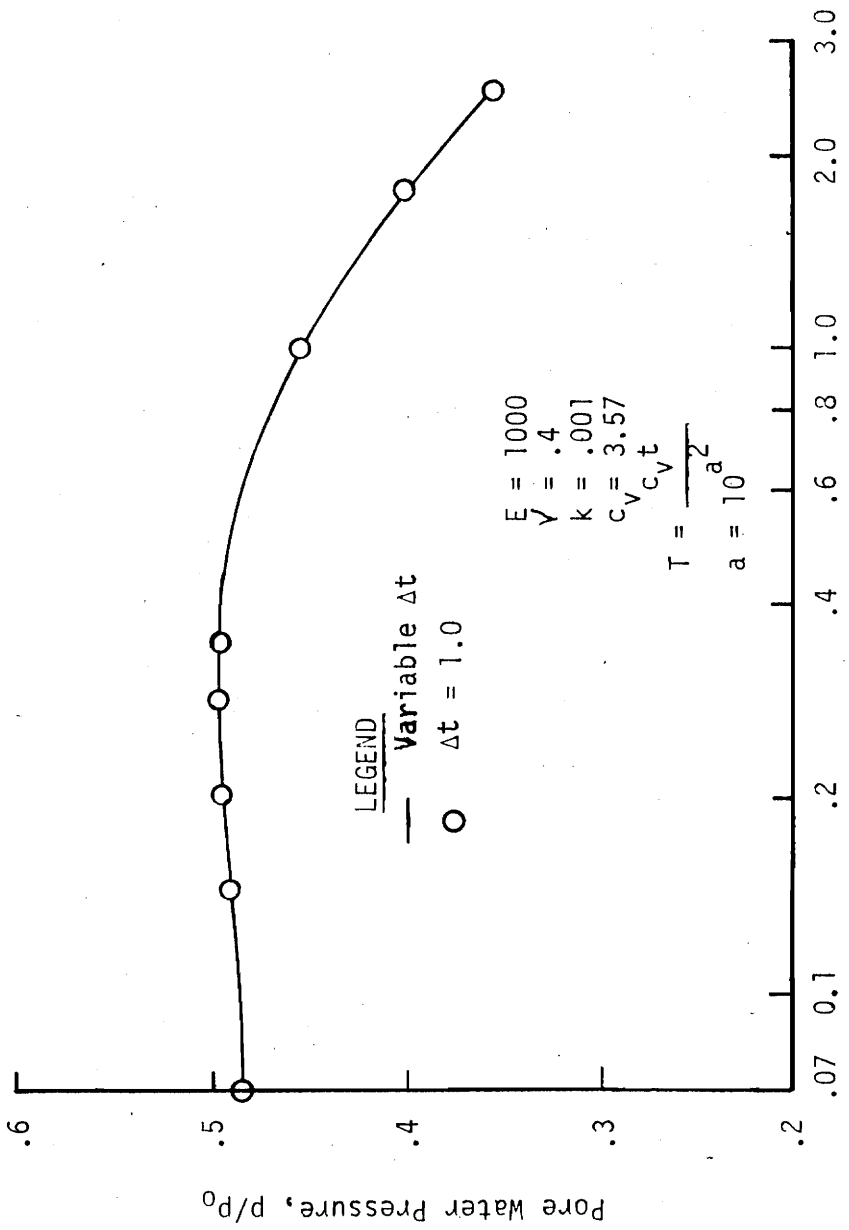

Figure 15 . Effect of Time Increment Δt on the Solution.

Chapter Five

CONSOLIDATION OF LAYERED SOILS

Finite Element formulation for 2-D consolidation has been usually applied to simple problems of one homogeneous soil layer, and little attempt has been made to analyze practical situations involving consolidation of multi-layered soils with greater variation of the elastic and permeability constants. These variations can pose computational difficulties, particularly at the interface between various soil layers. It is the intent of this chapter to examine the effects of the material parameters E and k on the consolidation process and to arrive at guidelines for the selection of these parameters for reliable answers.

In order to analyze this problem, a three layered soil system of clay-sand-clay was chosen. Figure 16 shows the material properties, boundary conditions and initial loading of the problem and Figure 17 shows the FE mesh used for the analysis. It may be noted that a refined mesh is used near the interfaces. A strip footing with a uniform loading, p_o = 1000 lbs, was selected arbitrarily and it was applied in a width a.

Variation in Permeability k

Pore pressure distributions at the center section for different ratios of k_r and for two times, t = 1.1 days and t = 21.1 days, are shown in Figures 18 and 19. Here K_r = permeability ratio = $\frac{k_2}{k_1}$ and $k_1 = k_3$, where k_1 = permeability coefficient for layer 1, k_2 = permeability coefficient for layer 2, and k_3 = permeability coefficient for layer 3.

The values used for permeability coefficient ratio were k_r = 1, 10, 10^2, 10^3, 10^4, 10^5, 10^6. The elastic material constants E and ν were assumed to be the same for all three layers: E = 85000.0 psf and ν = 0.3.

The values of $k_r = 10^4$, E = 85000.0 psf and ν = 0.3 were obtained for a field problem which is analyzed later on in this chapter. The pore pressure distributions appear reasonable for low values of k_r. For t = 1.1 days the pore pressure in layer 2 showed different distributions until a value of $k_r = 10^4$; for higher values of k_r, pore pressures remained essentially constant. For t = 21.1 days and beyond $k_r = 10^4$ some inaccuracy is observed in the bottom layer.

Figure 20 shows vertical settlement at the top node of the center section for different values of k_r at different time levels. It is observed that for higher values of k_r the magnitude of settlement is about the same while different values of settlements occur for lower values of k_r.

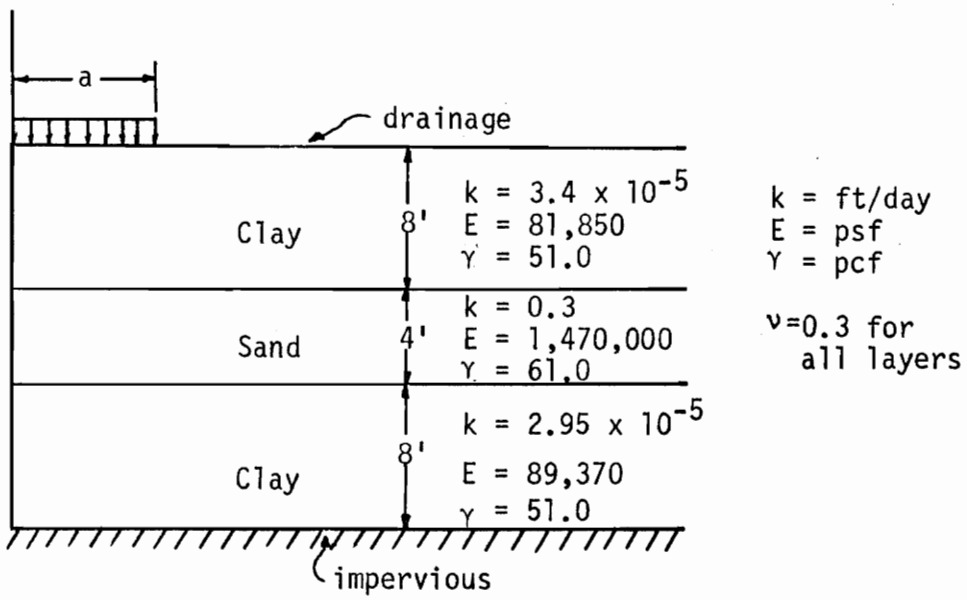

Figure 16. Two-Dimensional Three-Layered System.

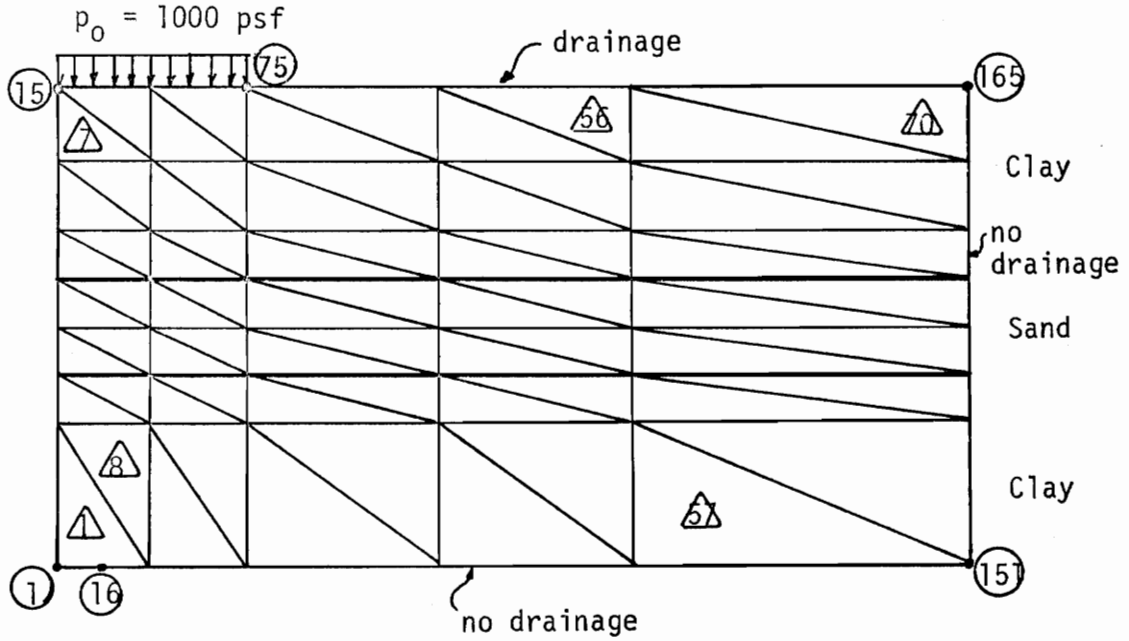

Total Number of Nodal Points = 165
Total Number of Elements = 70

Figure 17. Finite Element Mesh and Boundary Conditions.

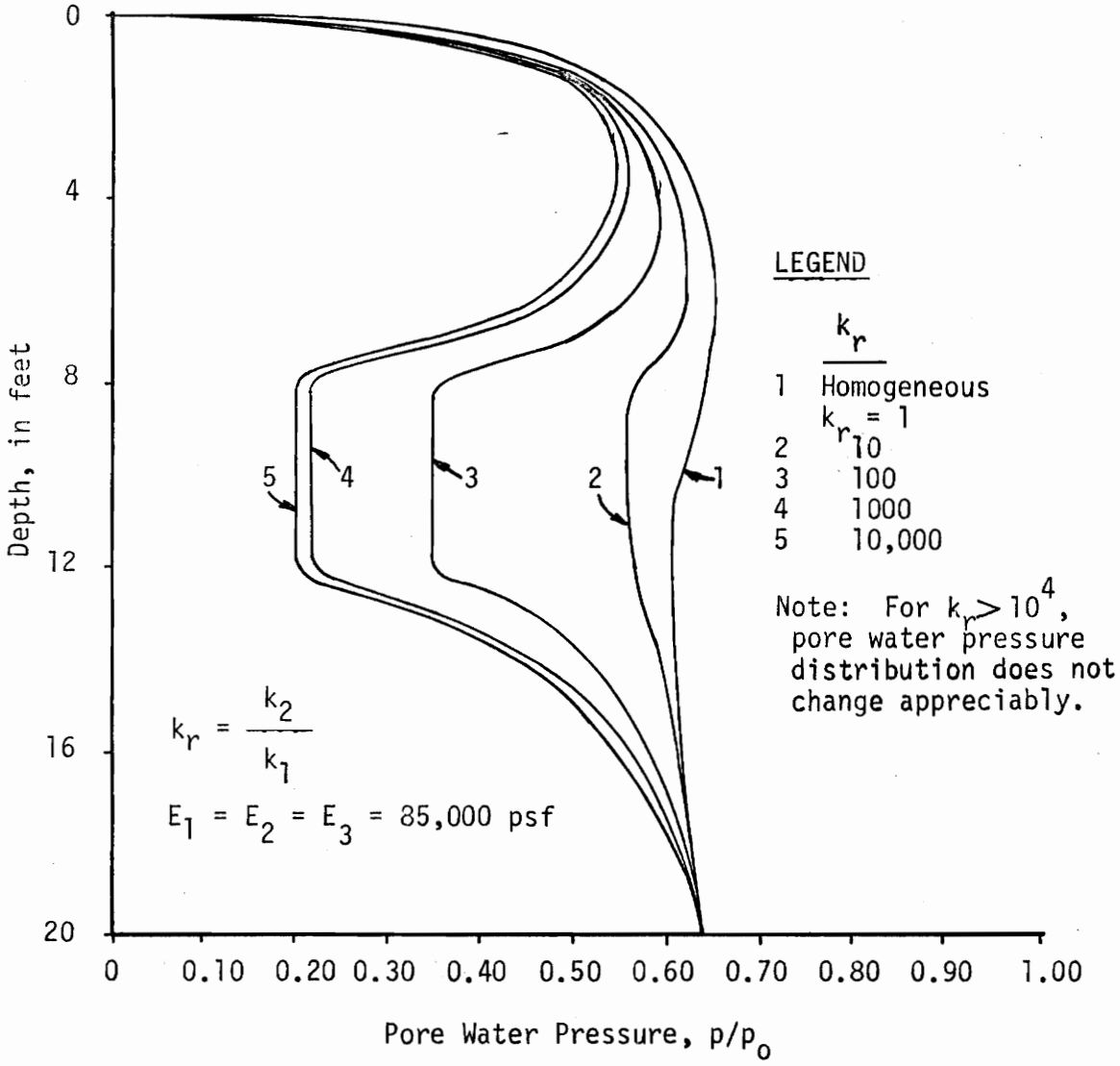

Figure 18. Distribution of Pore Water Pressure at Center Line for Different k_r, t = 1.1 days.

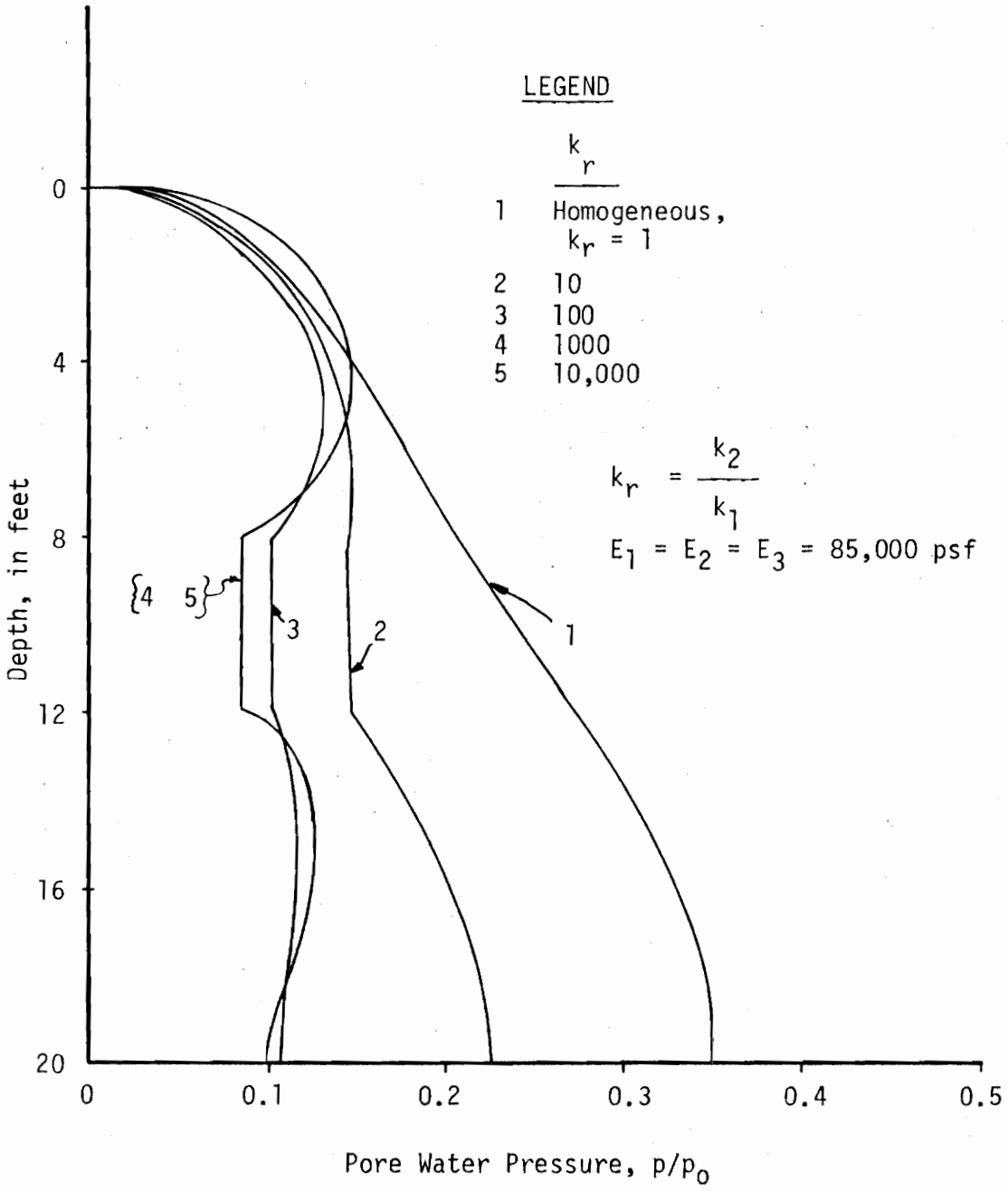

Figure 19. Distribution of Pore Water Pressure at Center Line for Different k_r, t = 21.1 days.

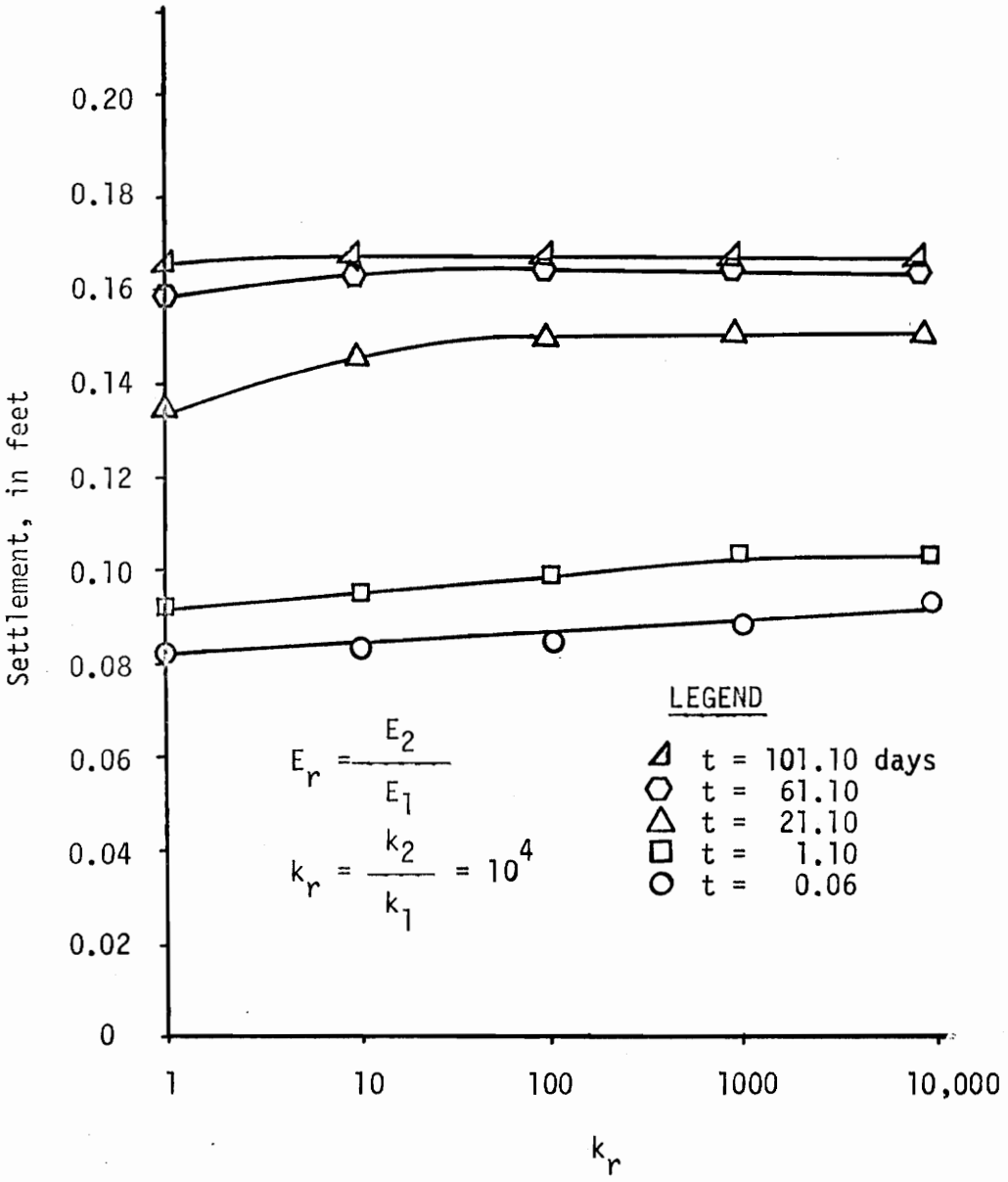

Figure 20. Time Settlement at Center Surface Node for Different k_r.

Variation of Elastic Modulus E

Pore water pressure distribution for different values of E_r were plotted for t = 1.1 days and 21.1 days as shown in Figures 21 and 22, respectively. $E_r = \frac{E_2}{E_1}$, where E_1 = Modulus of Elasticity for layer 1, E_2 = Modulus of Elasticity for layer 2, and E_3 = Modulus of Elasticity for layer 3.

The values of E_r used in the analysis are shown in Figures 21 and 22; Permeability ratio k_r = 1.0 was used and E_3 was taken to equal E_1. It is observed that in early stages, at t = 1.1 days, there is irregularity and inaccuracy in the solution. Figure 22 shows that beyond a value of $E_r = 10^3$, the numerical solution can become irregular and inaccurate. Time settlements of the surface node along the center line shown in Figure 23, as expected, were decreased as the values of E_r increased.

Similar analyses were performed for $k_r = 10^4$ and shown in Figures 24, 25, and 26. It can be seen that the results become irregular and lose accuracy for a value of E_r larger than 10^4. From Figure 26 it can be seen again as expected that the settlements decrease as the value of E_r increases.

Comment:

It can be observed then that the FE formulation used for this analysis gives satisfactory results for a wide range of E_r and k_r ratios. However, for ratios greater than $k_r = 10^4$ and $E_r = 10^3$ the results can become irregular.

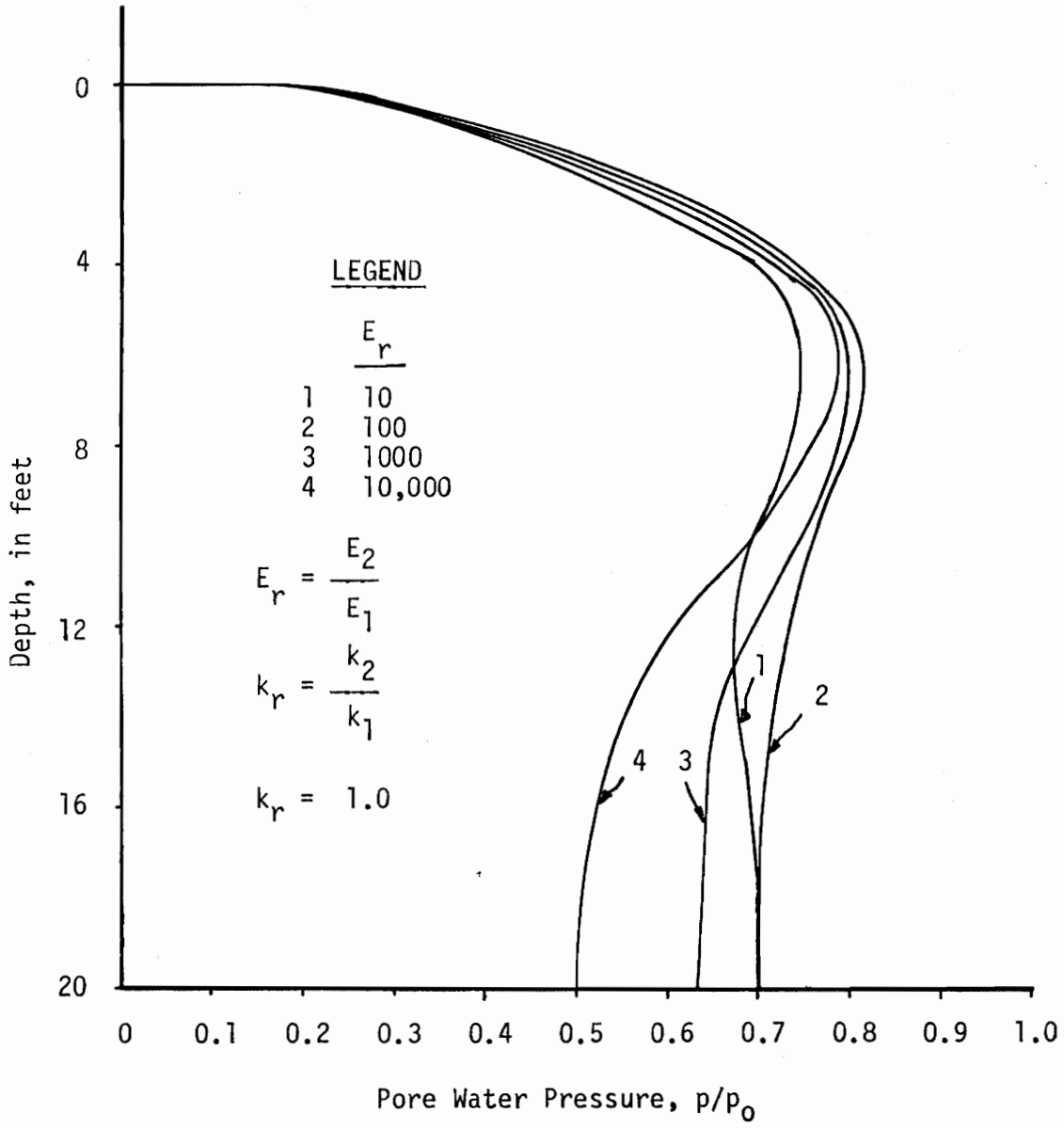

Figure 21. Distribution of Pore Water Pressure at Center Line for Different E_r, t = 1.1 days, and k_r = 1.0.

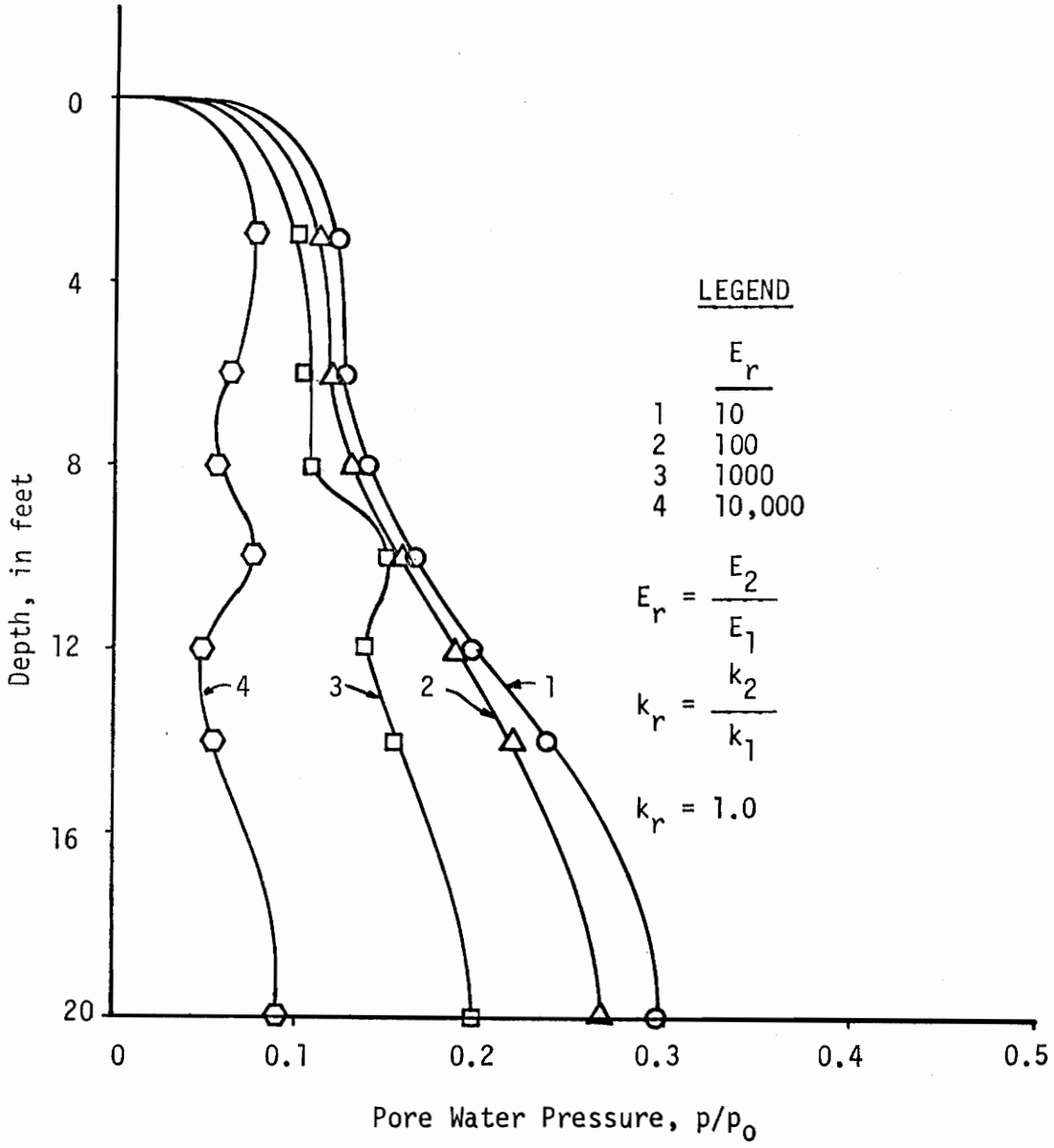

Figure 22. Distribution of Pore Water Pressure at Center Line for Different E_r, t = 21.1 days, and k_r = 1.0.

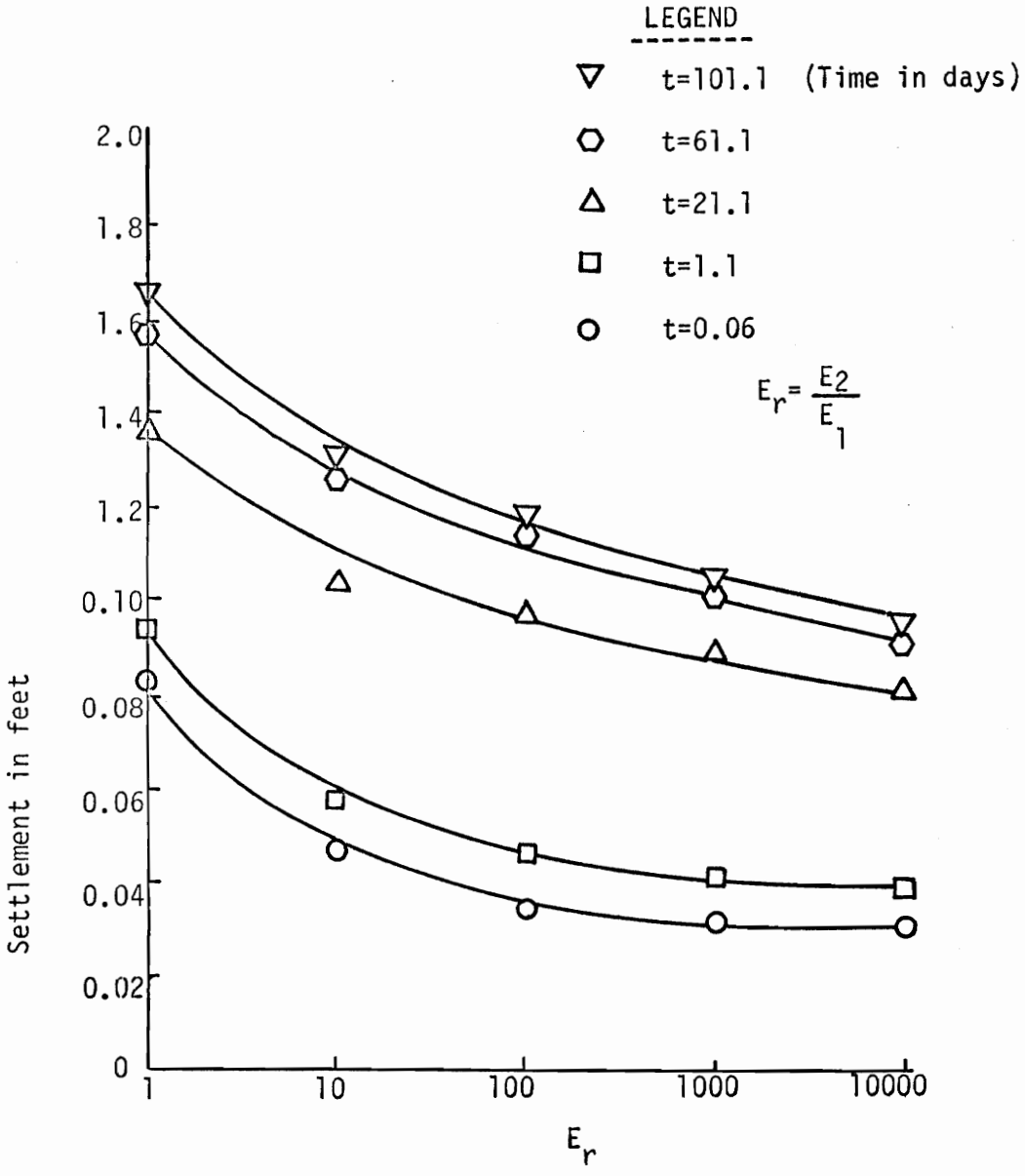

Figure 23. Time Settlement at Center Surface Node for Different E_r and K_r=1.0 .

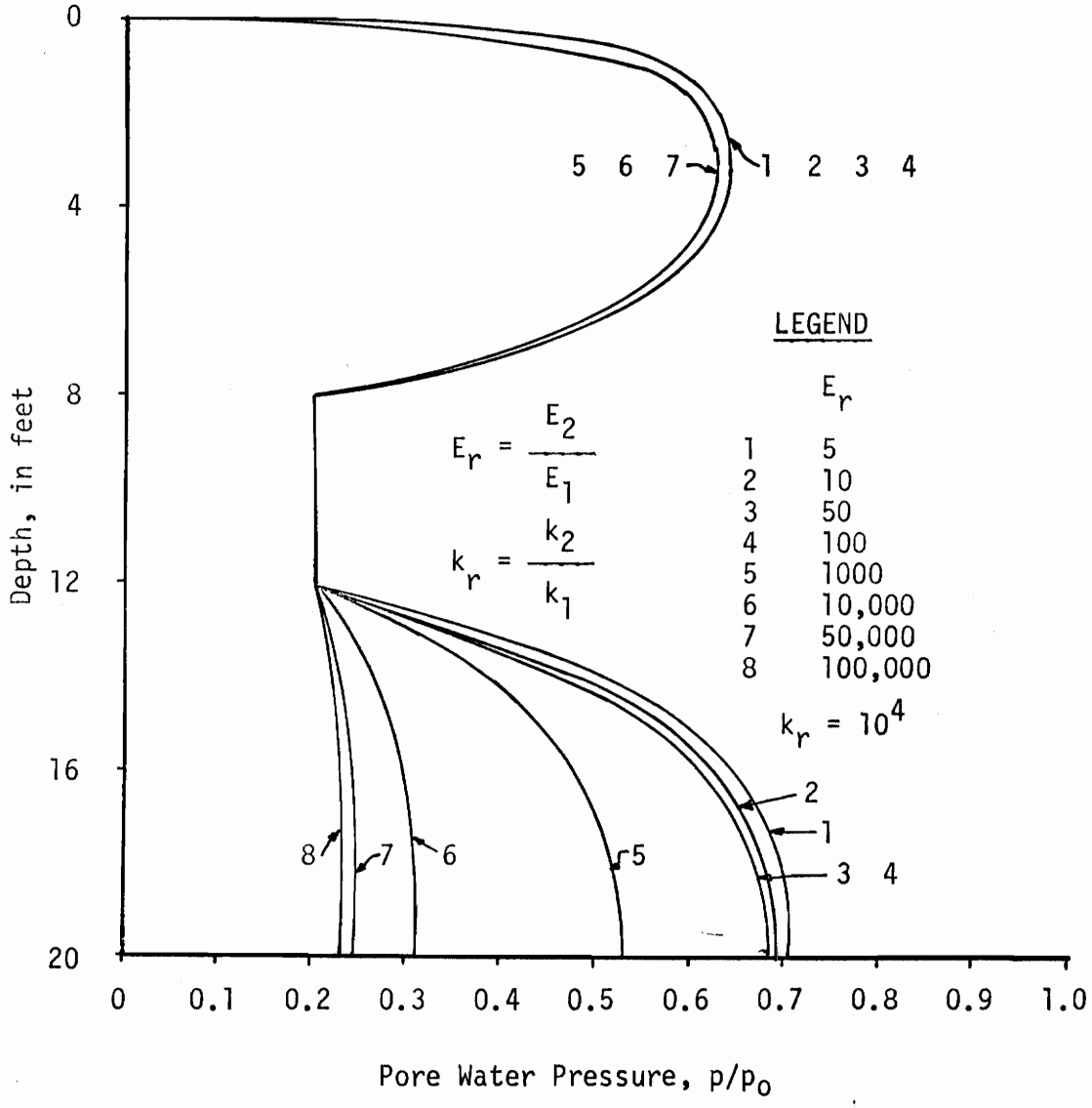

Figure 24. Distribution of Pore Water Pressure at Center Line for Different E_r, t = 1.1 days, and $k_r = 10^4$.

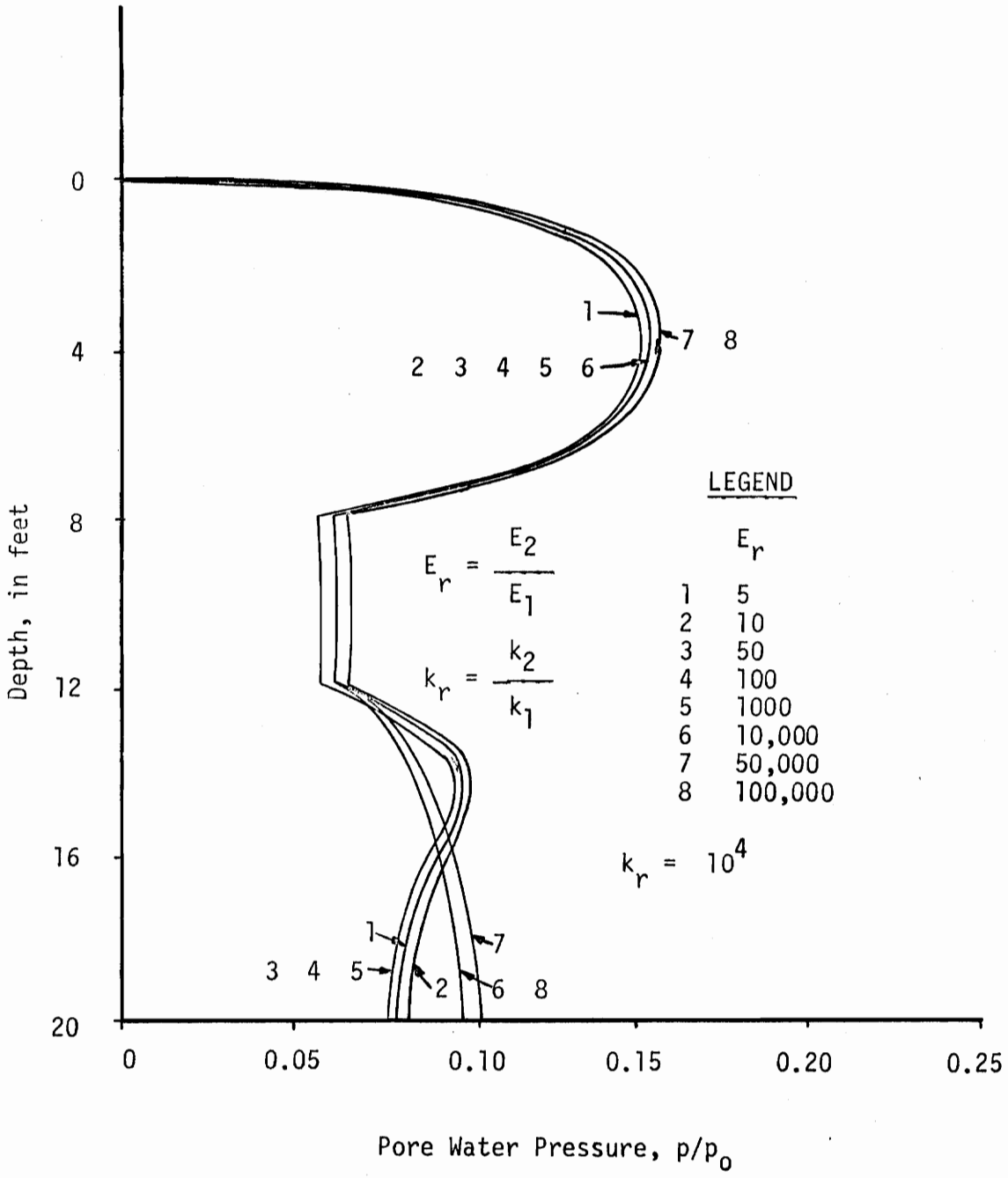

Figure 25. Distribution of Pore Water Pressure at Center Line for Different E_r, t = 21.1 days, and $k_r = 10^4$.

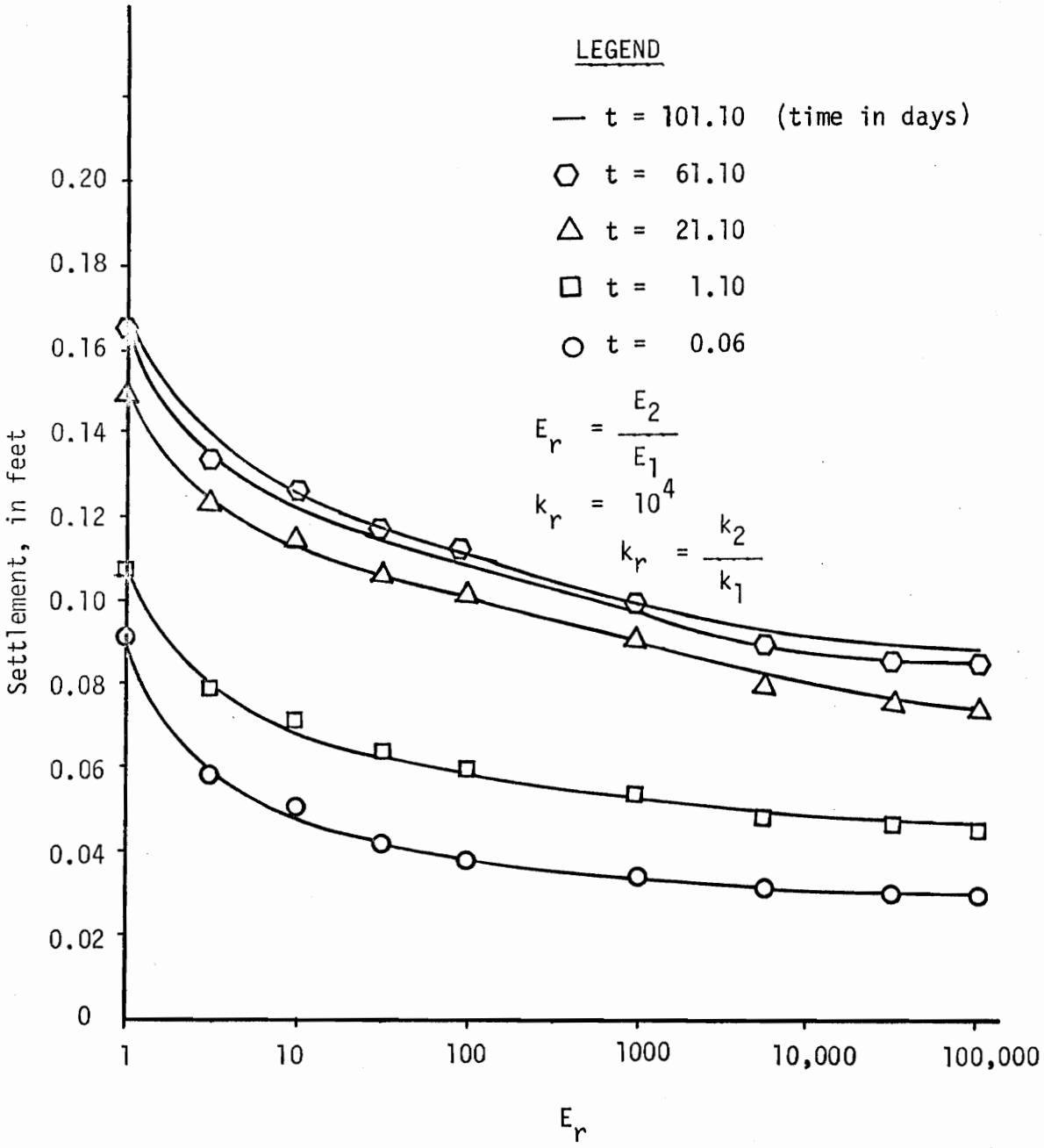

Figure 26. Time Settlement at Center Surface Node for Different E_r and $k_r = 10^4$.

Analysis of Field Problem

The FE method was applied on a four-layered soil system under an embankment which was proposed as a protection around a structure in the ocean, Saxena [25].

Figure 27 shows the geometry and the material properties, E, ν, k and γ used in the analysis. The material properties were determined from extensive laboratory tests, and varied widely, particularly the value of k for the four layers. The values of $\bar{E}$ and $\bar{k}$ indicate the average values for each layer.

Figure 28 shows the loading, boundary conditions and the finite element mesh used. Pore pressure distribution at two time levels and two vertical sections within the FE mesh are shown in Figure 29. The time dependent settlement for the top section under the loading is shown in Figure 30. The maximum settlement was 1.171 feet for the section under node number 176. Figure 31 shows the time settlement for each layer of the soil system. The results of this analysis appear very reasonable. Field measurements of pore pressures and settlement for the above problem were not available and hence it is not possible to compare the results.

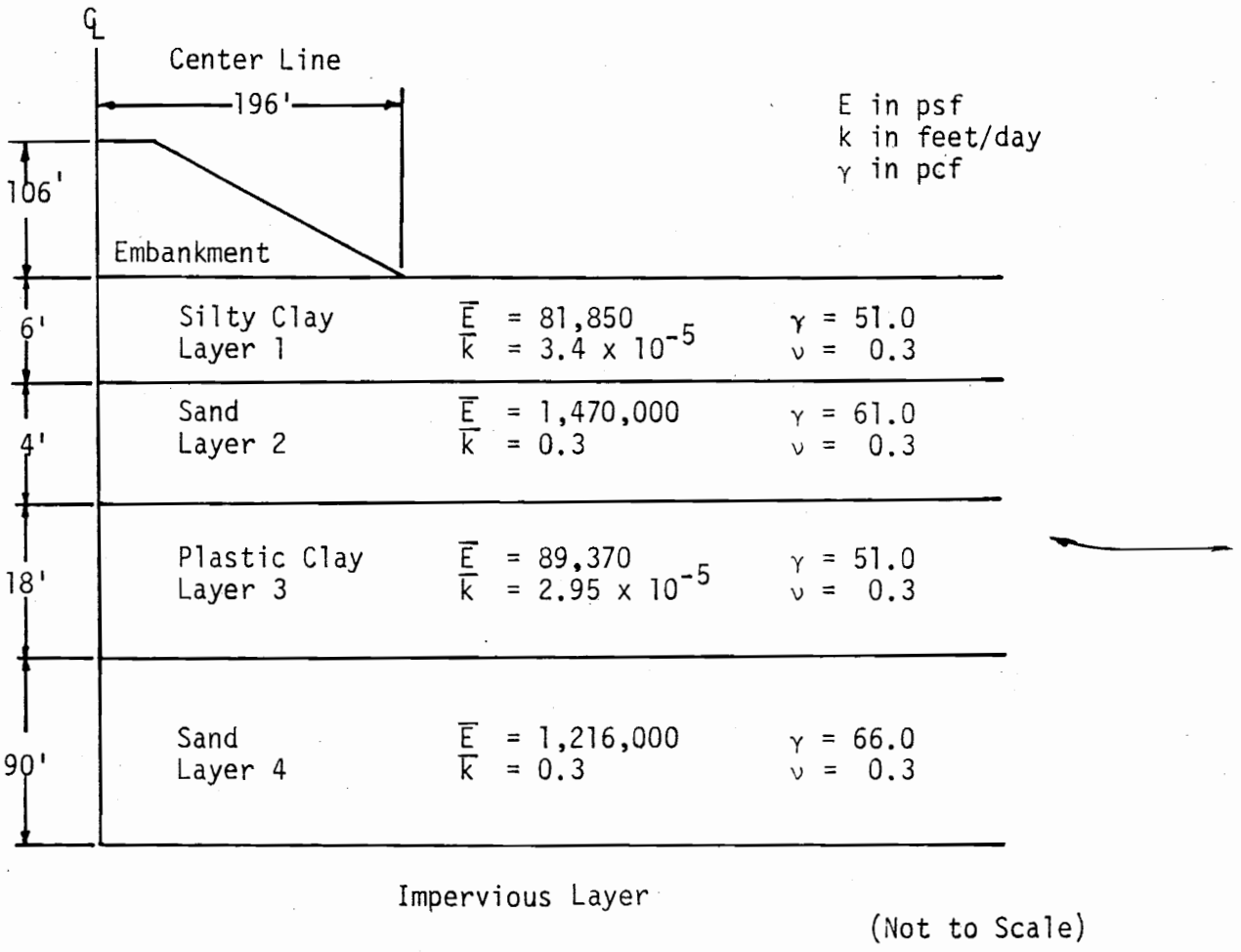

Figure 27. Field Problem, Geometry and Material Properties.

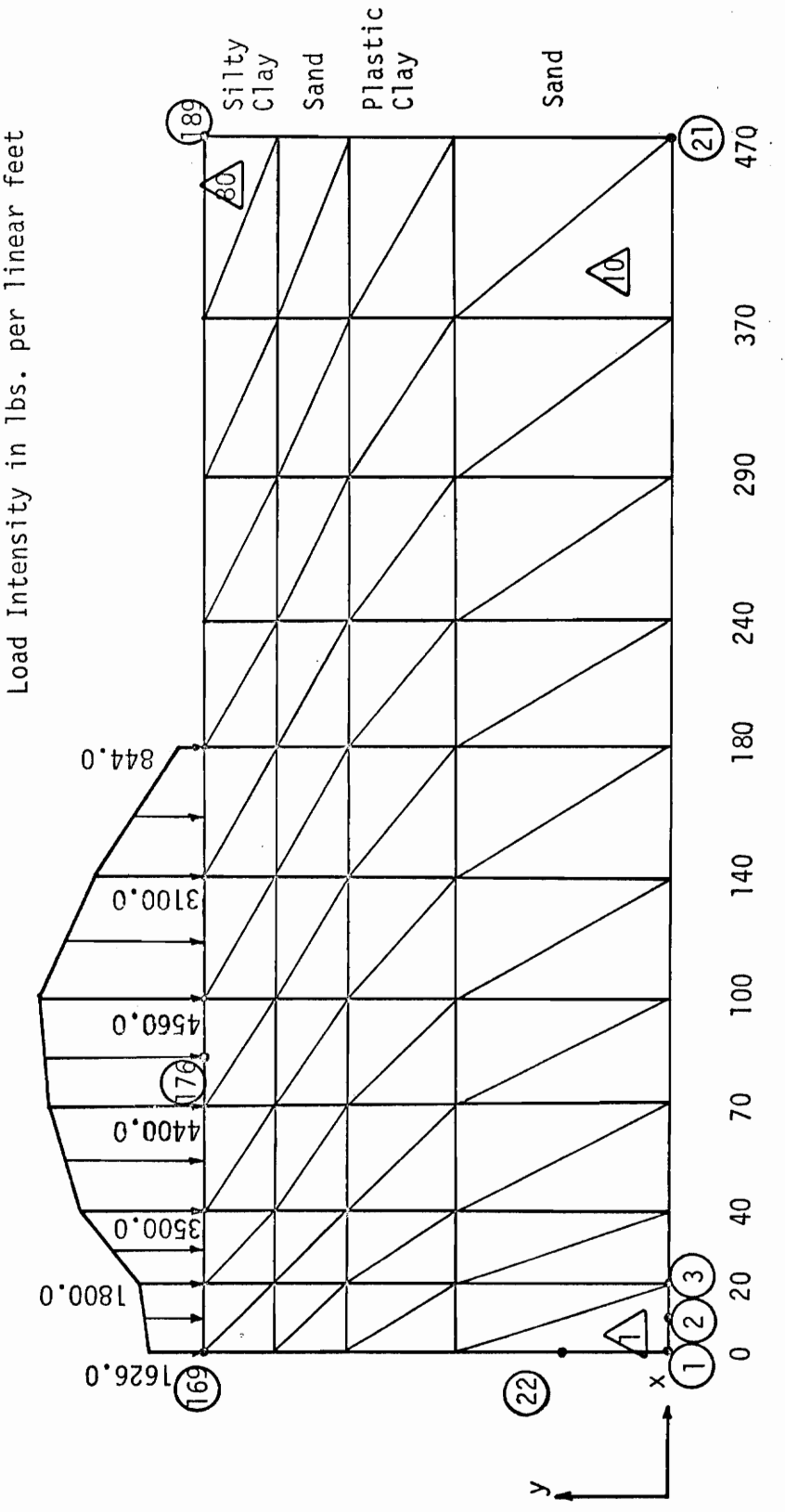

Total Number of Nodal Points = 189
Total Number of Elements = 70

Figure 28. Finite Element Mesh and Loading used for the Analysis of a Field Problem.

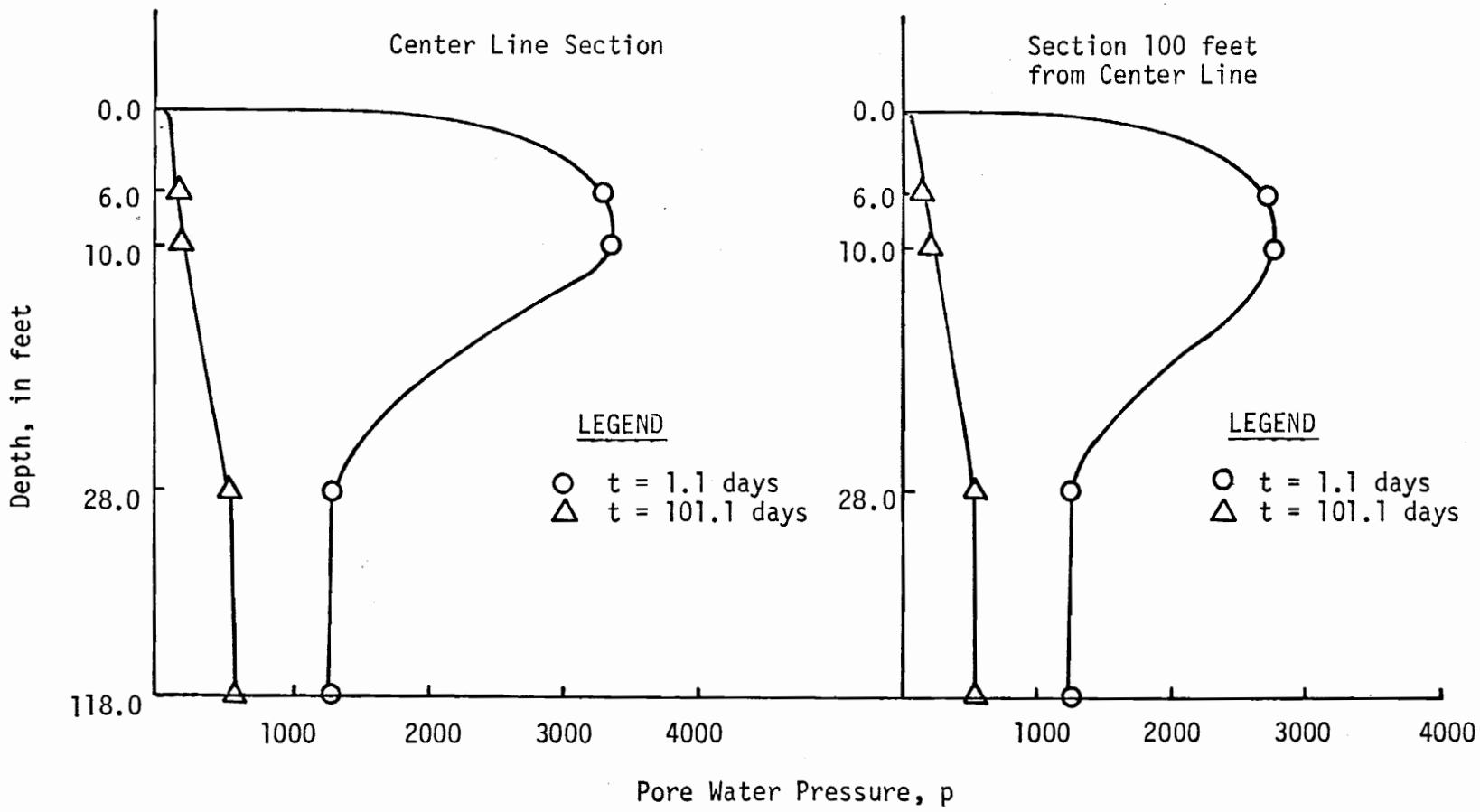

Figure 29. Pore Water Pressure Distribution along the Center Line and a Section 100 feet from Center Line.

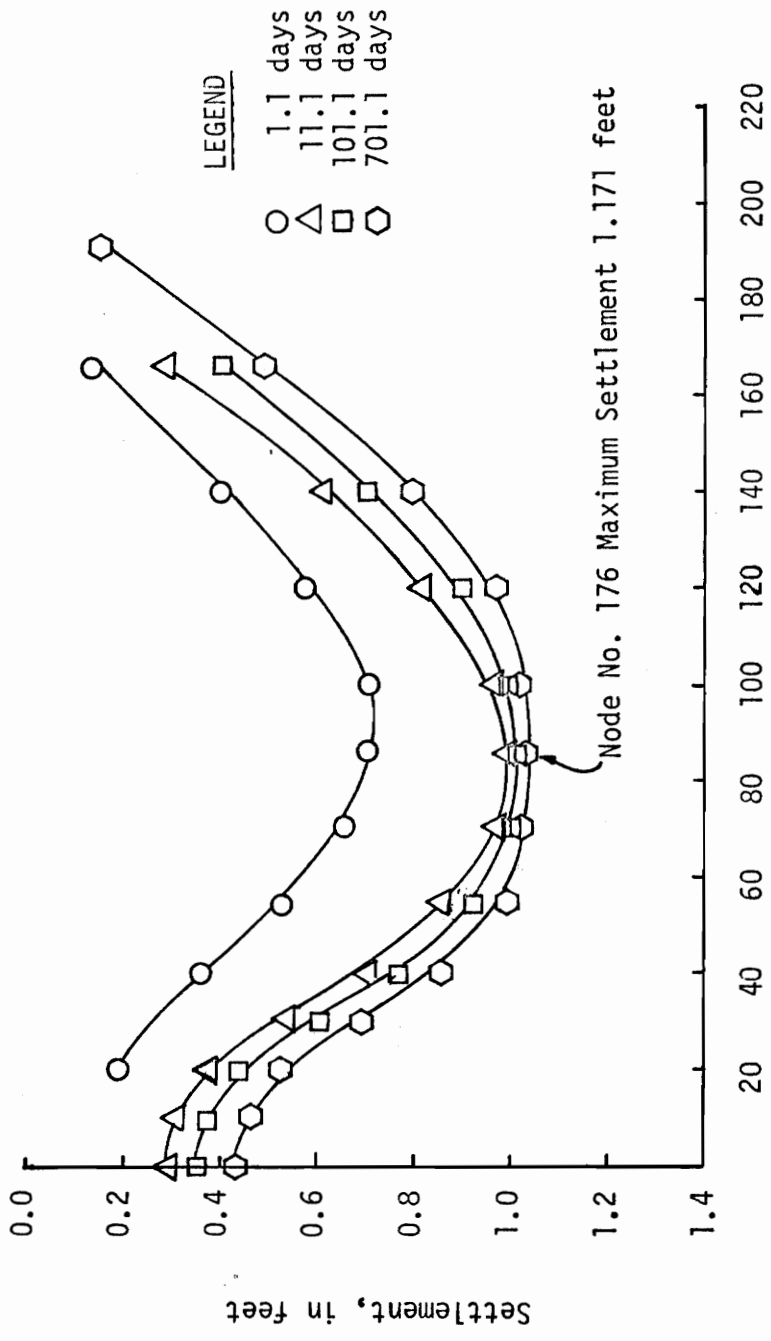

Figure 30. Time Settlement for the Surface Top Nodes.

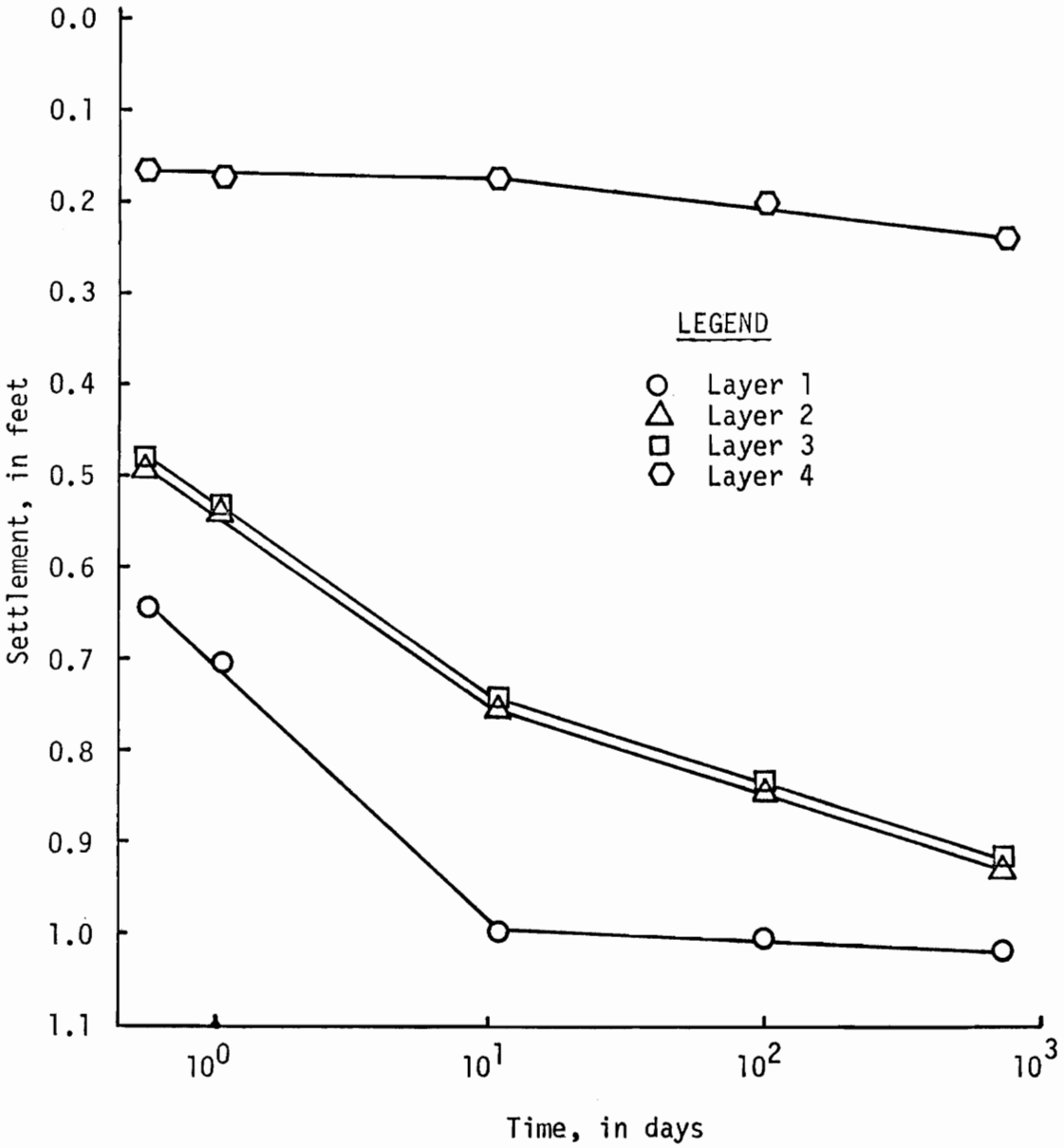

Figure 31. Time Settlement for the Four Layers at a Section 85 feet from Center Line.

Chapter Six

CONSOLIDATION OF ANISOTROPIC SOILS

In most of the papers on the one- and two-dimensional consolidation, soil has been treated as a homogeneous isotropic material having the same strength and permeability in both vertical and horizontal directions. In nature, many of the soils are anisotropic because of the mode of original deposition, the stress changes after deposition or both. Consequently, the strength and permeability of some soils will vary with the direction of the plane with respect to physical vertical. It is important therefore to examine the effect of strength and permeability anisotropy on the rate of consolidation.

Types of Anisotropy

1. Strength Anisotropy. It describes the directional variation of strength and it has been found experimentally to be of two kinds. In the first type the horizontal strength is higher than the vertical. This was observed in the heavily overconsolidated London clay. In the second type of strength anisotropy, the vertical strength is higher than the horizontal, and experimental results on an overconsolidated clay deposit in Welland, Ontario, Lo [17] showed a ratio c_H/c_V varied from 0.8 to 0.64, where c_H = horizontal strength, and c_V = vertical strength. Strength anisotropy has also been considered by Yokoo et al [33].

In order to examine the effect of the strength anisotropy on the rate on consolidation, ratios of the material elastic constants, Young's Modulus E and Poisson's ratio ν, were introduced in the linear relationship

between stresses and strain,

$$\{\sigma\} = [C]\{\varepsilon\} \tag{21}$$

where [C] is the elasticity matrix containing the appropriate material properties.

For the plane strain and isotropic material the matrix [C] is given by

$$[C] = \frac{E(1-\nu)}{(1+\nu)(1-2\nu)} \begin{bmatrix} 1 & \nu/1-\nu & 0 \\ \nu/1-\nu & 1 & 0 \\ 0 & 0 & (1-2\nu)/2(1-\nu) \end{bmatrix} \tag{22}$$

From Figure 32, taking the y-axis perpendicular to the strata, E_1, ν_1, and G_1 are associated with the behavior in the x-axis and E_2, ν_2, and G_2 with the behavior in the y-axis. Taking $\frac{E_1}{E_2} = n$ and $\frac{G_2}{E_2} = m$, where G = elastic shear modulus and $m = \frac{1}{2(1+\nu)}$, the matrix for plane strain becomes, Zienkiewicz, [34],

$$[C] = \frac{E_2}{(1+\nu_1)(1-\nu_1-2n\nu_2^2)} \begin{bmatrix} n(1-n\nu_2^2) & n\nu_2(1+\nu_1) & 0 \\ n\nu_2(1+\nu_1) & (1-\nu_1^2) & 0 \\ 0 & 0 & n(1+\nu_1)(1-\nu_1-2n\nu_2^2) \end{bmatrix} \tag{23}$$

The effect of strength anisotropy on consolidation was investigated for different values of $\frac{E_x}{E_y}$ ratios. The results of this parametric study are discussed in the next section.

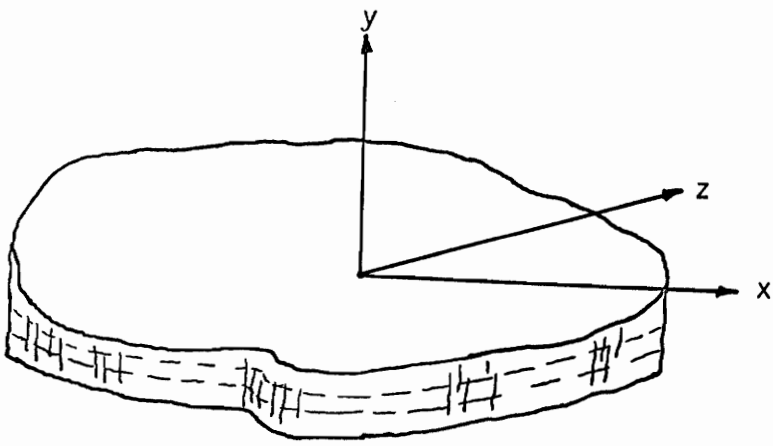

Figure 32. Stratified or a Transversely-Isotropic Material.

Parametric Study for Strength Anisotropy

The first part of this parametric study was made for the type of anisotropy where the vertical strength is higher than the horizontal (Welland clay). The geometry of the problem and the material properties are shown in Figure 33. The permeability ratio retained constant $\frac{k_H}{k_V}$ = 1.0. Two ratios of $\frac{E_x}{E_y} = \frac{1}{10}$ and $\frac{1}{100}$ were investigated.

Plots of pore pressure versus a depth ratio H/a were made for $T = 2 \times 10^{-5}$, 1.1×10^{-2}, 5.01 at the center section. (Figures 34, 35, and 36). T is an adjusted time factor equal to $c_v t/a^2$ where c_v = 1.0, t = real time, and a = the width of the load. C_v is taken as constant so the real time t (hours) can be computed. At early stages of consolidation, lower horizontal strength decreased considerably the pore pressures in the bottom part of the soil mass (while under the load the reduction was much less). It should be noted that in the top section under the load for $\frac{E_x}{E_y} = \frac{1}{100}$ the pore pressure is higher than that from $\frac{E_x}{E_y} = \frac{1}{10}$. This can be due to the fact that the percent consolidation settlement is lower for $\frac{E_x}{E_y} = \frac{1}{100}$ at $T = 2 \times 10^{-5}$ and 1.1×10^{-2}. The pore water pressure concentration directly under the load at early stages of consolidation, could be contributed to the Mandel-Cryer effect and it was also noted by Schiffman et al [26], and Valliapan et al [32]. At later stages of consolidation, T = 5.01, Figure 36, it can be seen that the pore pressures are lower for the ratio of $\frac{E_x}{E_y} = \frac{1}{10}$ and $\frac{1}{100}$. Figure 37 shows percent consolidation settlement versus T. As it can be expected the rate of consolidation settlement was smaller for higher values of $\frac{E_x}{E_y}$.

The second part of this parametric study was for the strength anisotropy where the horizontal strength is higher than the vertical. It was not possible to analyze values of the ratio $\frac{E_x}{E_y} > 1.7$, however, ratios of $\frac{E_x}{E_y} < 1.7$ have been obtained in many field and laboratory observations; ratio $\frac{E_x}{E_y} = 1.6$ was observed for London clay. Figures 38 and 39 show pore water pressure distribution for the center line section at $T = 1.1 \times 10^{-2}$ and 5.01. It is observed that the pore water pressure distribution for $\frac{E_x}{E_y} = 1.7$ is higher than $\frac{E_x}{E_y} = 1.0$ particularly for $T = 1.1 \times 10^{-2}$. From Figure 40 it can be observed that the vertical strength being lower than the horizontal decreases the rate of consolidation settlement at early stages but increases it at later stages of consolidation. The consolidation settlement in Figure 37 and 40 at T=0.0 would be zero. The large settlements at early stages of consolidation is due to the high permeability constant k=0.001 cm/sec used in the analysis.

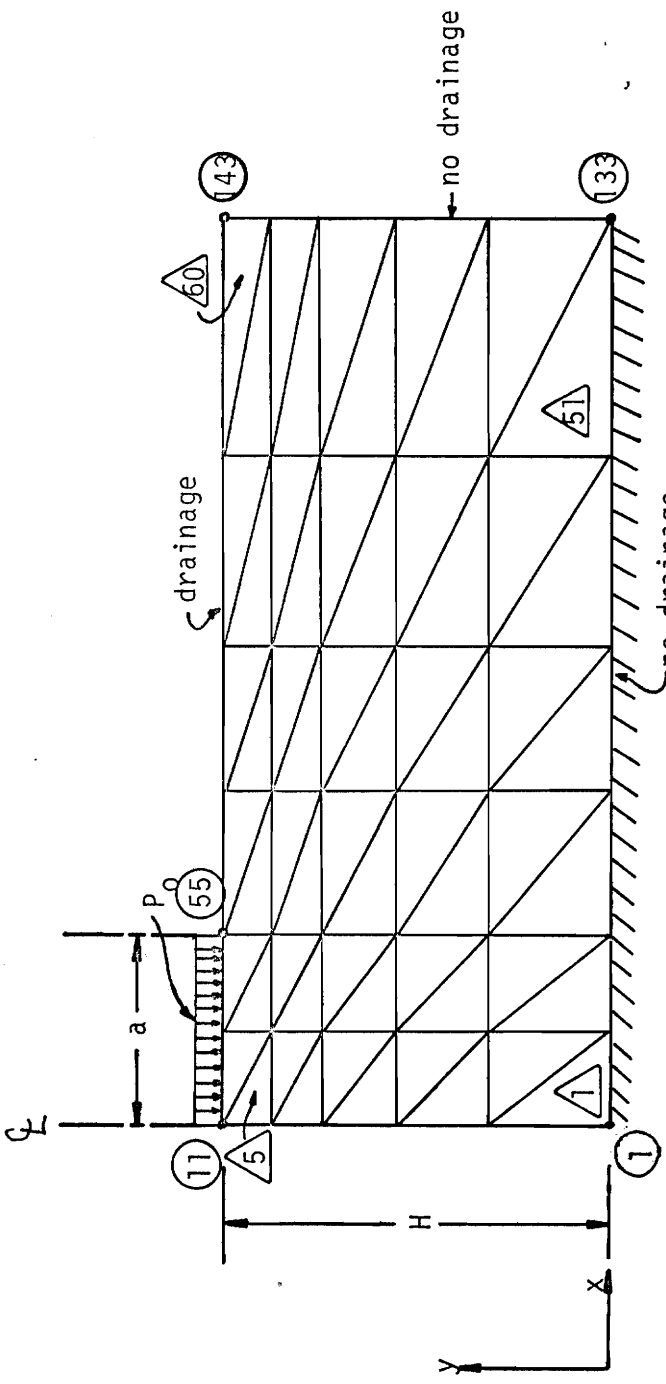

Total Number of Nodal Points = 143
Total Number of Elements = 60

Figure 33. Problem Geometry and Finite Element Mesh Representation used for the Consolidation Analysis of Anisotropic Soils.

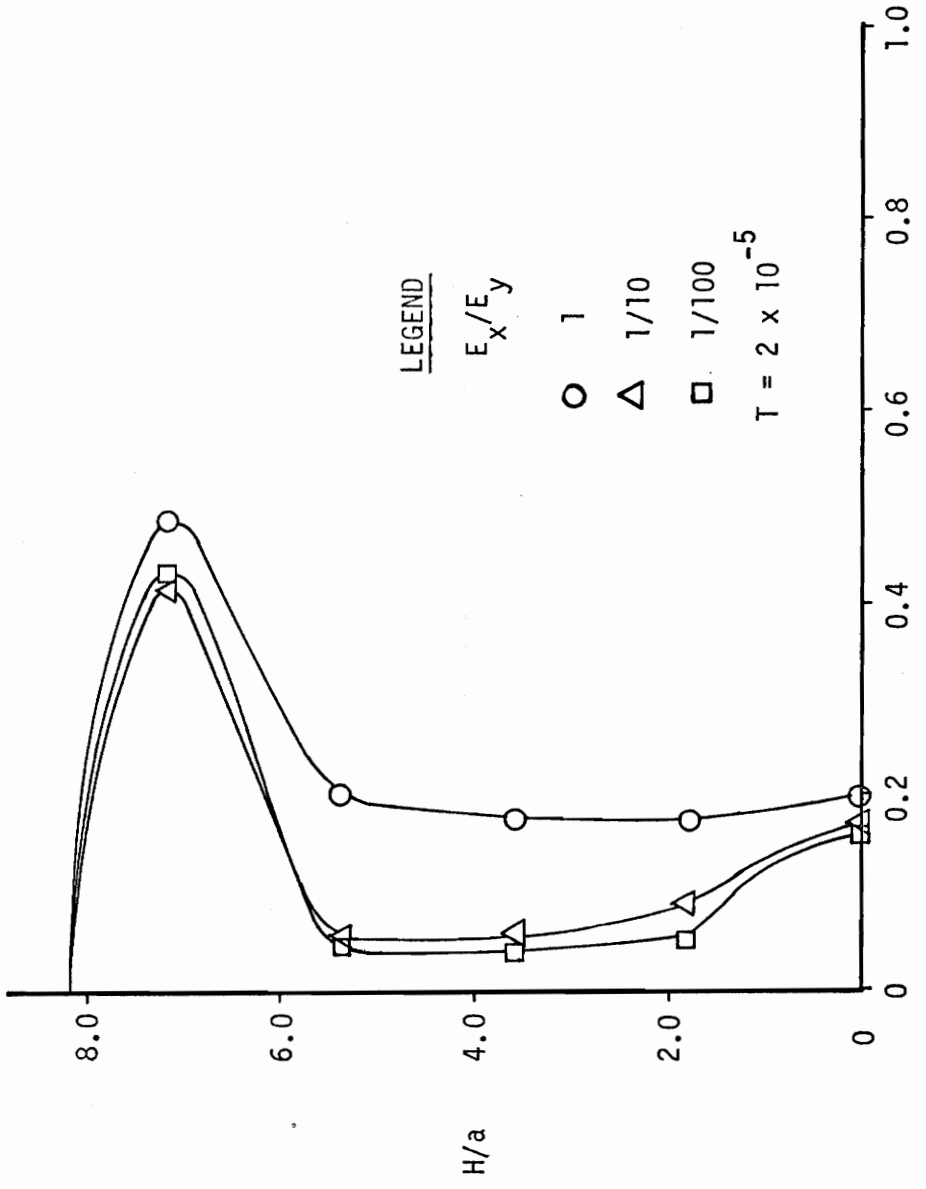

Figure 34 . Pore Water Pressure Distribution at Center Line for Different Ratios of E_x/E_y, $T = 2 \times 10^{-5}$

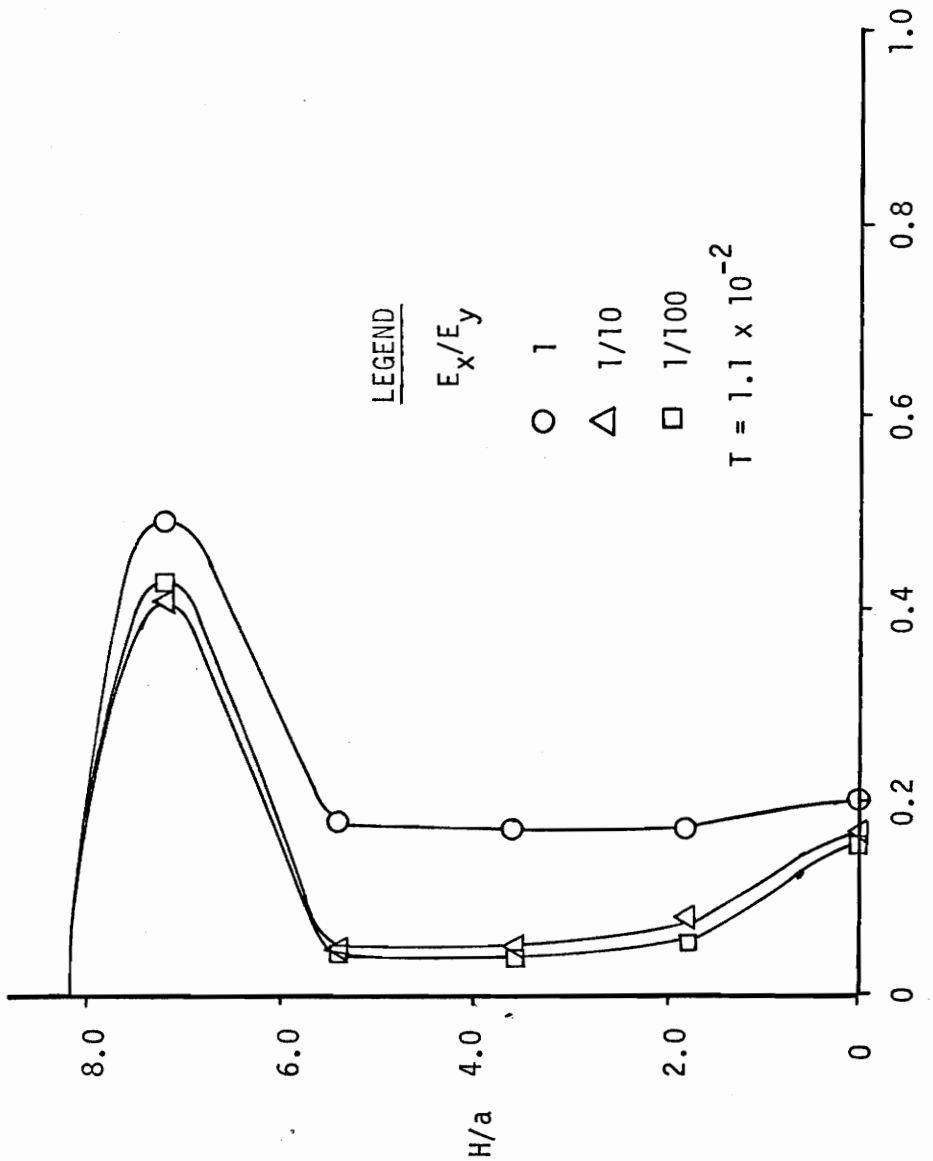

Figure 35. Pore Water Pressure Distribution at Center Line for Different Ratios of E_x/E_y, $T = 1.1 \times 10^{-2}$.

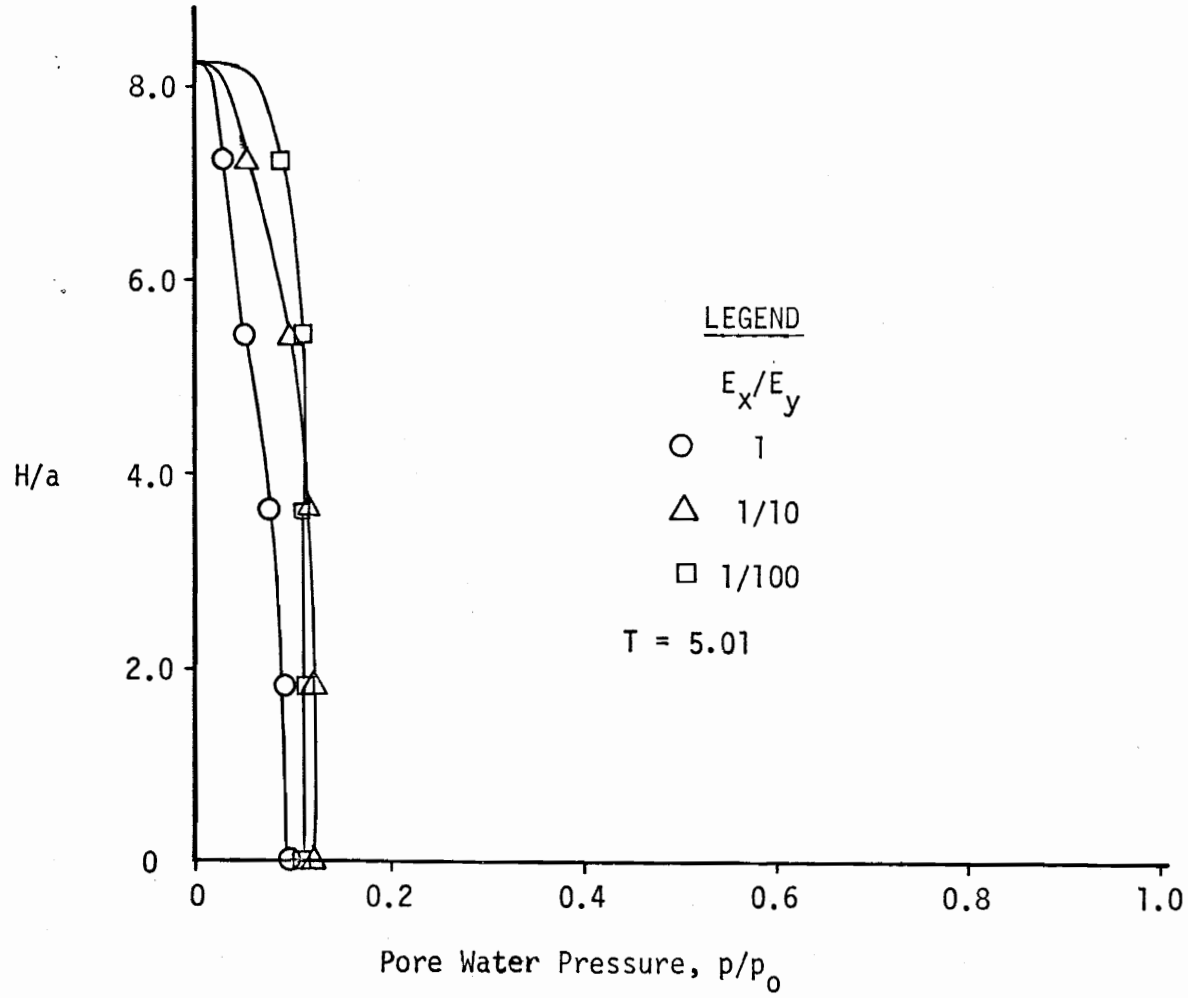

Figure 36. Pore Water Pressure Distribution at Center Line for Different Ratios of E_x/E_y, T = 5.01.

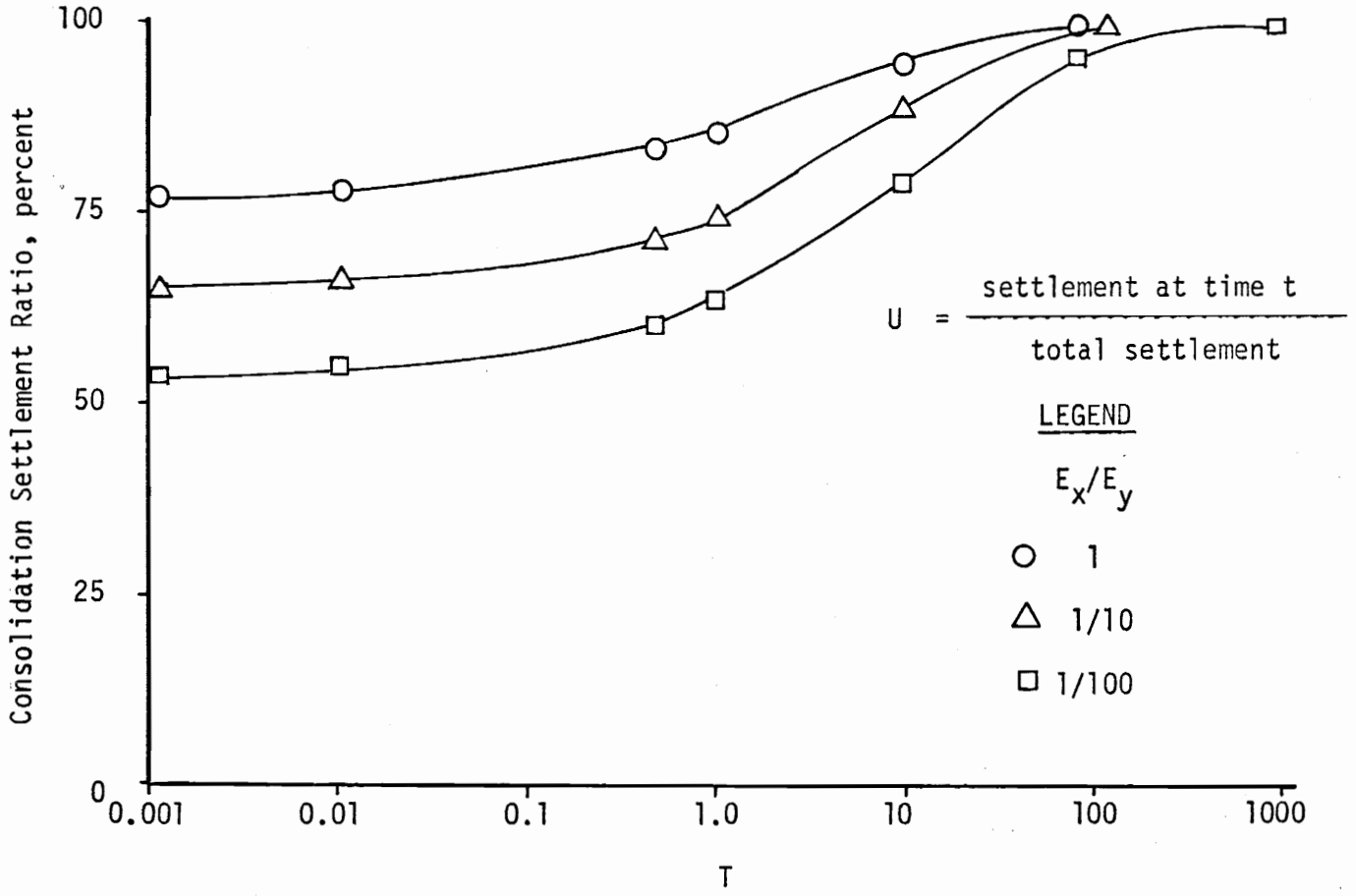

Figure 37 . Percent Consolidation Settlement Ratio (U) versus T for Different Values of $E_x/E_y \leq 1.0$.

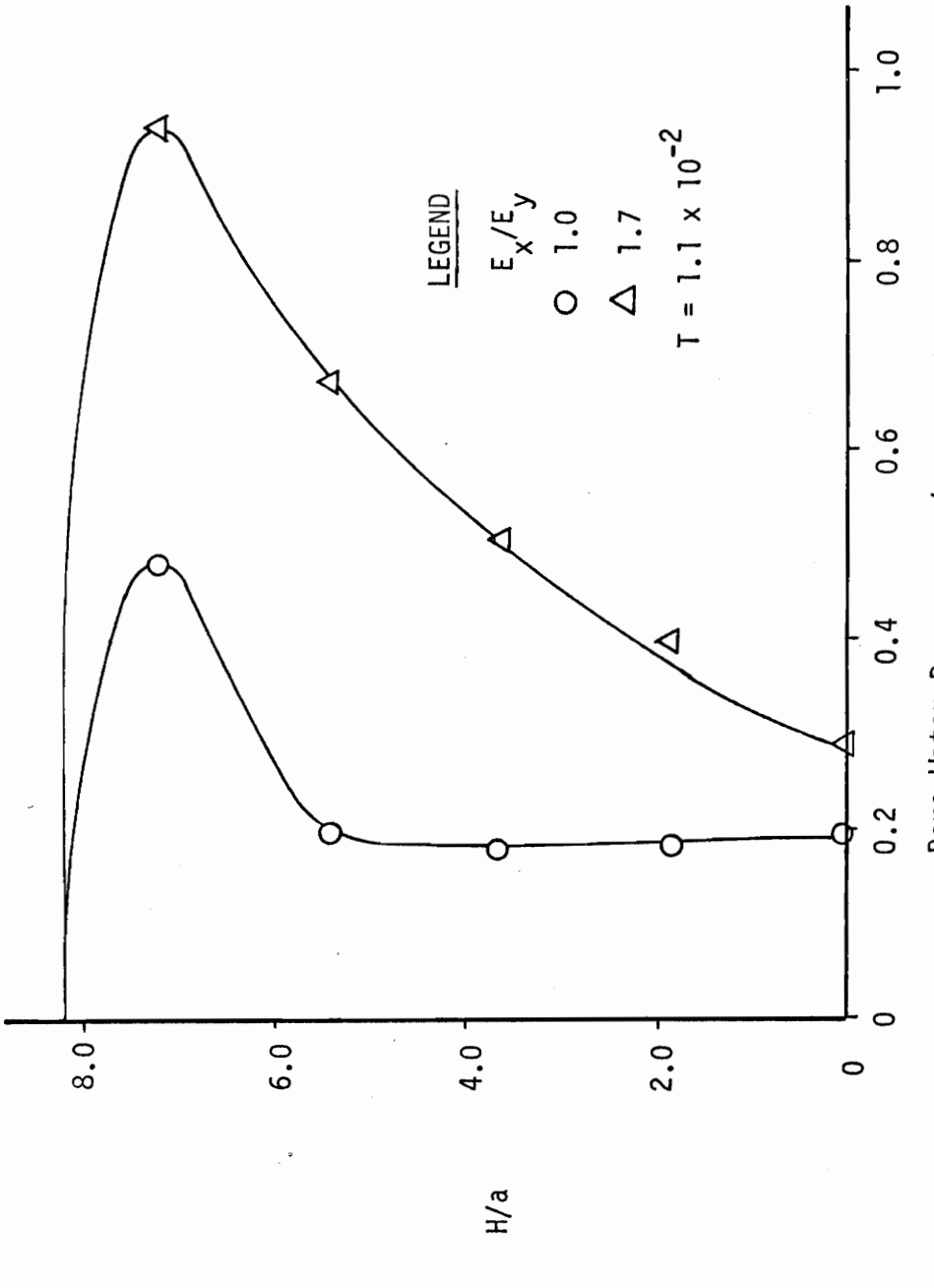

Figure 38 . Pore Water Pressure Distribution at Center Line for Different Ratios of E_x/E_y, T = 1.1 x 10^{-2}.

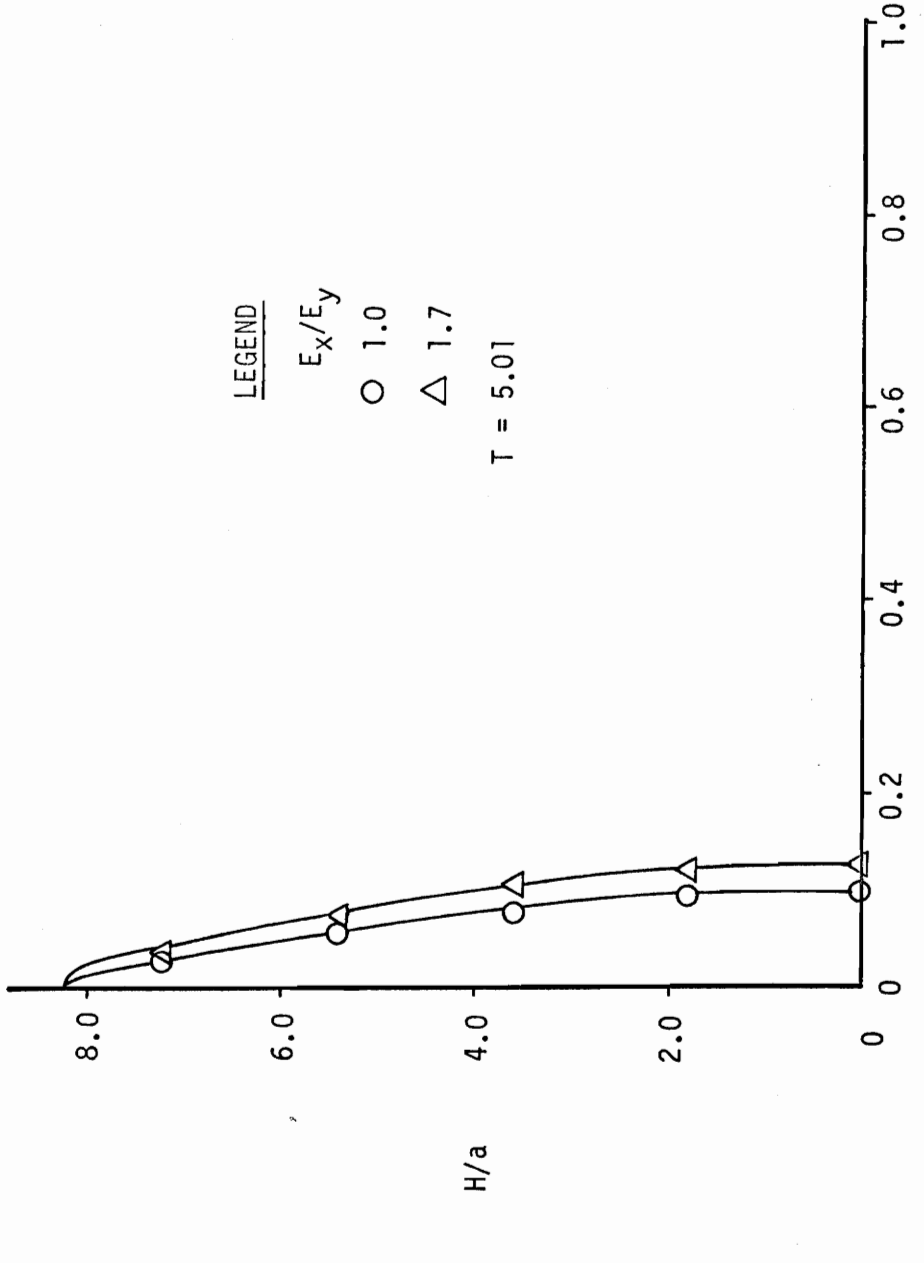

Figure 39. Pore Water Pressure Distribution at Center Line for Different Ratios of E_x/E_y, T = 5.01.

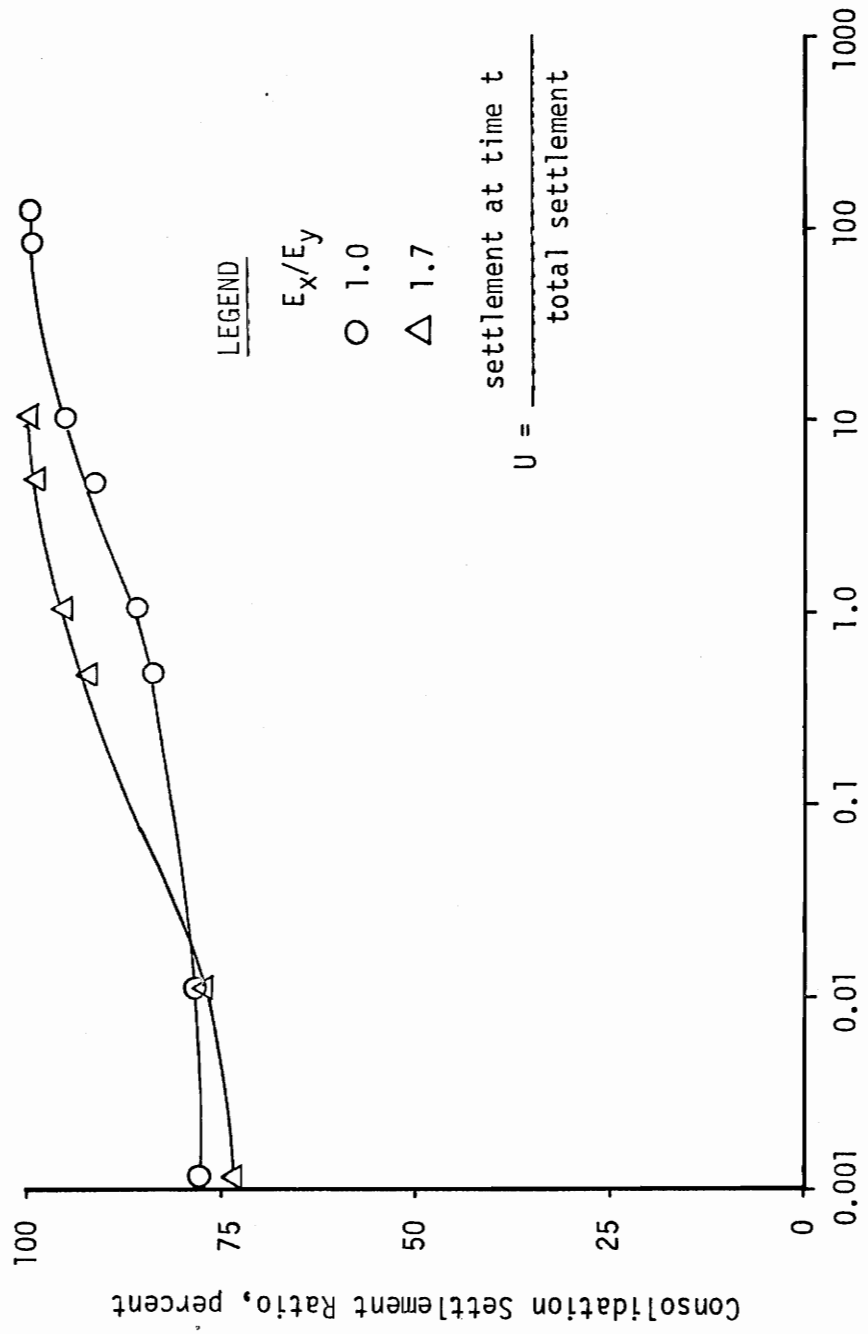

Figure 40. Percent Consolidation Settlement Ratio (U) versus T for Different Values of $E_x/E_y \geq 1.0$.

2. Anisotropic Permeability

The directional variation of permeability of cohesive soils has been investigated theoretically and experimentally and it has been found that the horizontal permeability is higher than the vertical $\frac{k_H}{k_V} \geq 1.0$, where using Figure 32, $k_H = k_x$ = horizontal permeability, and $k_V = k_y$ = vertical permeability.

The effect of the permeability anisotropy on the rate of consolidation has been investigated in this study by making computer runs with different ratios of $\frac{k_H}{k_V}$. The results of the parametric study are discussed below.

Parametric Study for Permeability Anisotropy

Computer runs with a ratio of horizontal to vertical permeability $\frac{k_H}{k_V}$ of 1, 10 and 100 were made. The elastic material properties were kept constant; $E_x = E_y = 1000$ and $\nu = 0.4$. The study was made using the geometry and material constants shown on Figure 33. Three plots of pore pressure distribution for the center section are shown in Figures 41, 42 and 43 for $T = 1.1 \times 10^{-2}$, 2.0×10^{-5}, and 5.01, respectively.

From Figure 41 it can be observed that in the early stages of consolidation there is pore water pressure concentration in the top region of the soil mass, and directly under the load. This pore water pressure concentration as it was explained earlier could be contributed to the Mandel-Cryer effect. At early times of consolidation, high horizontal permeability, k_H, allows the pore water pressures to drain horizontally and thus the rate of consolidation is accelerated. At later times of consolidation, Figures 42 and 43, the pore water pressures dissipate in

the vertical direction towards the top and are higher for the values of $\frac{k_H}{k_V}$ = 10. and 100. From Figure 44 it can be observed that for higher values of $\frac{k_H}{k_V}$ the rate of consolidation is decreased at late times of the consolidation process. The rate of consolidation settlement was determined for the top node of the center section of the problem.

A similar parametric study using the FE method was made by Christian and Boehmer [6] and Ladd and Wissa [16] and their results are in good agreement with the ones obtained in this study.

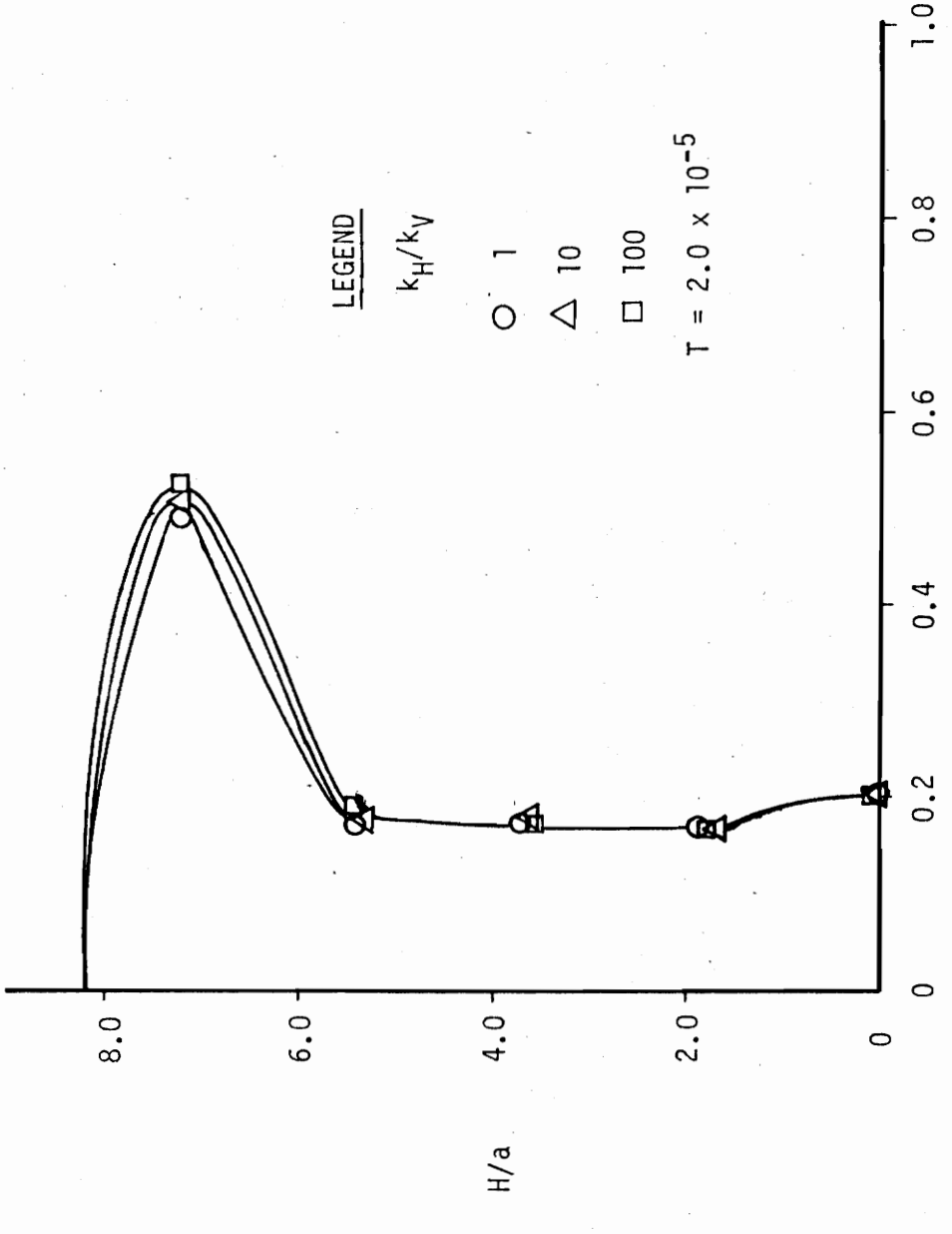

Figure 41 . Pore Water Pressure Distribution at Center Line for Different Ratios of $k_H/k_V \geq 1.0$. T = 2.0 x 10^{-5}.

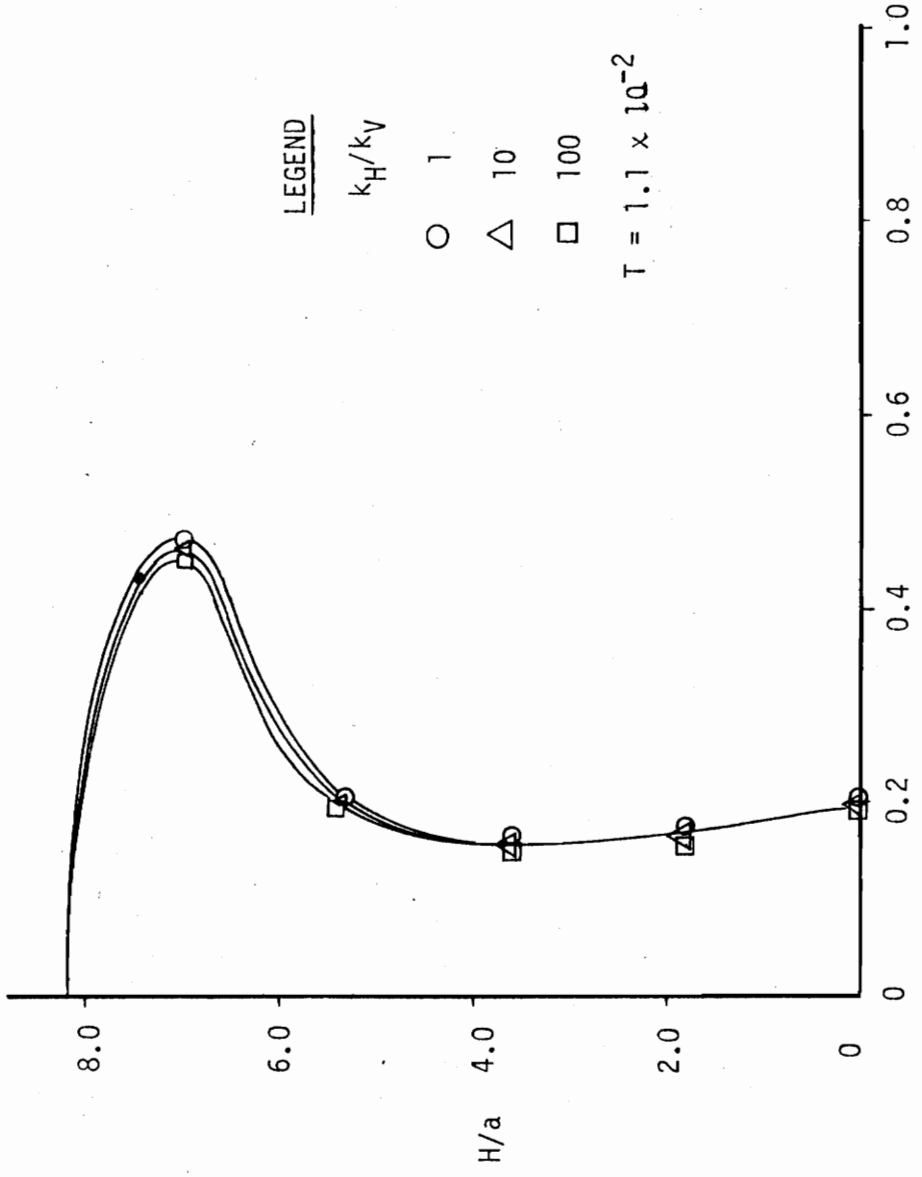

Figure 42 . Pore Water Pressure Distribution at Center Line for Different Ratios of $k_H/k_V \geq 1.0$. $T = 1.1 \times 10^{-2}$.

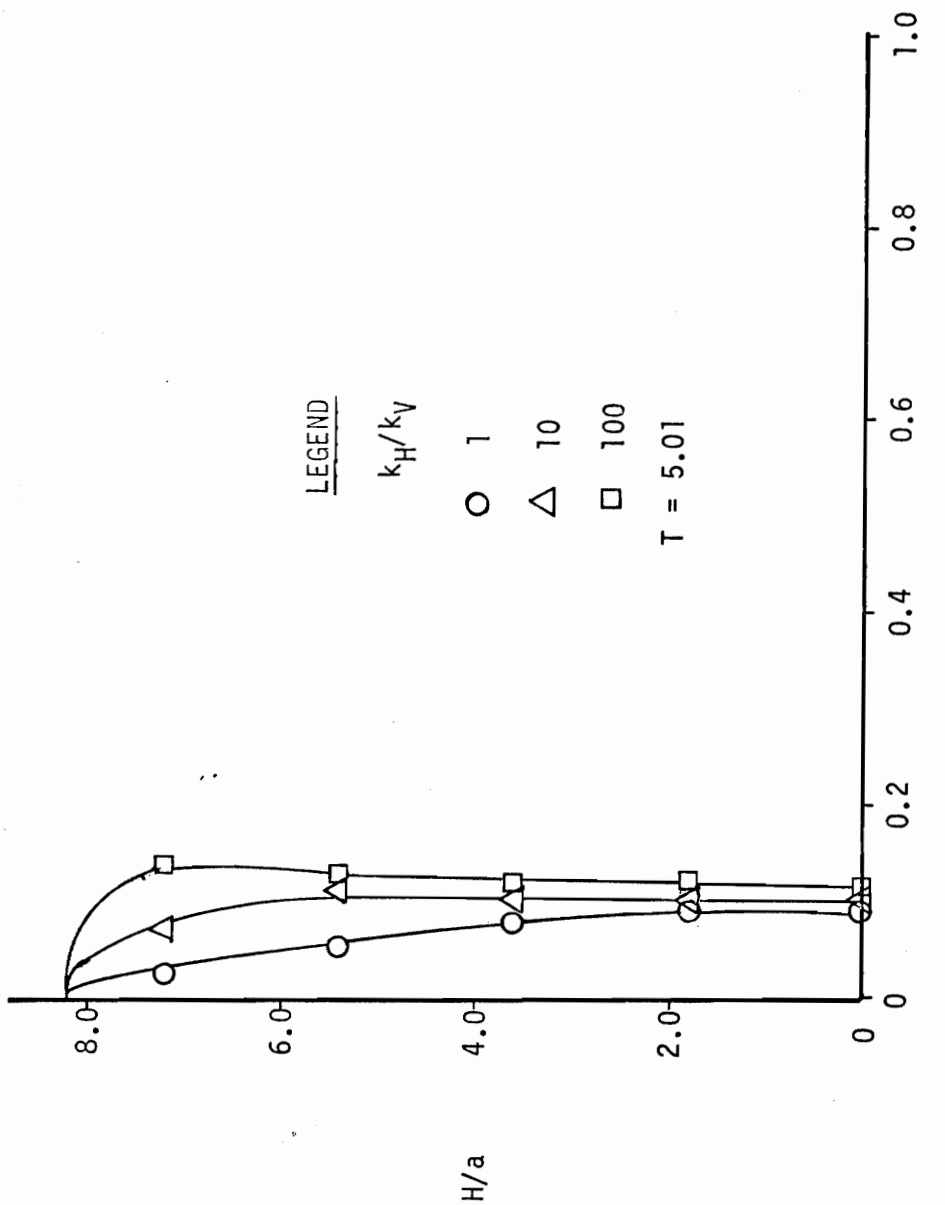

Figure 43 . Pore Water Pressure Distribution at Center Line for Different Ratios of $k_H/k_V \geq 1.0$. T = 5.01.

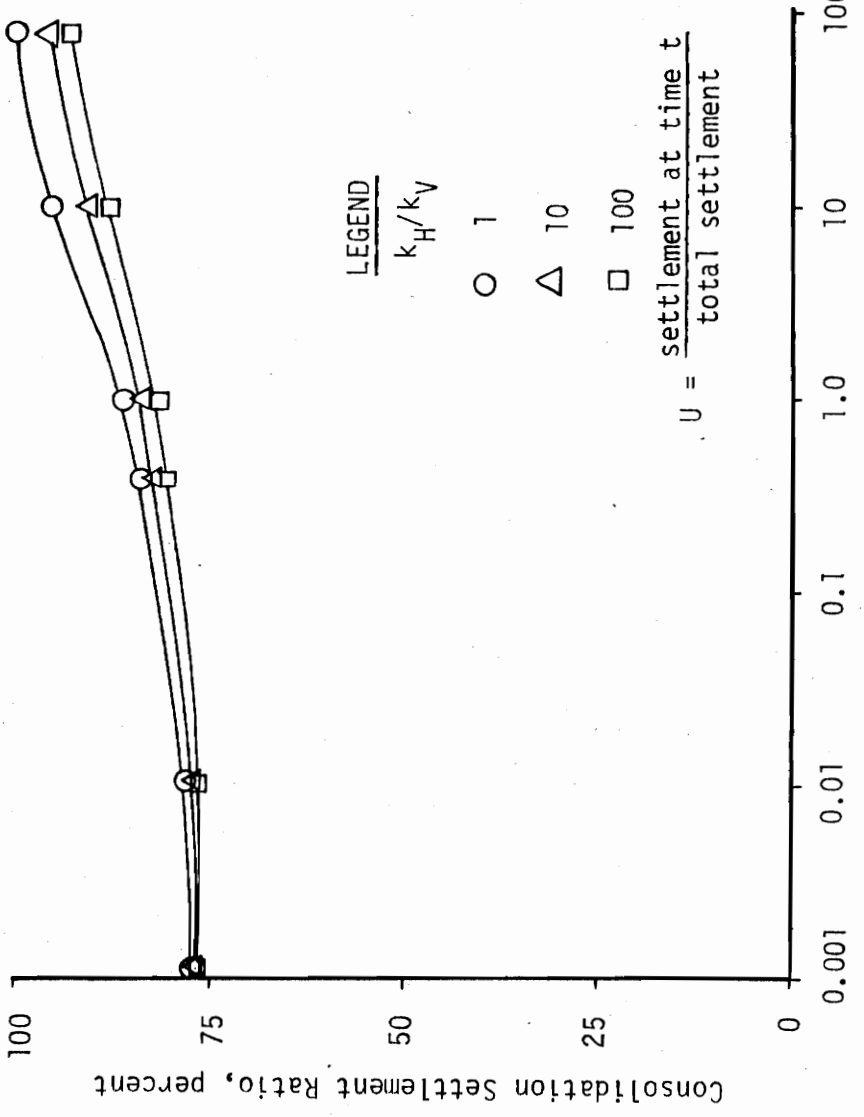

Figure 44. Percent Consolidation Settlement Ratio (U)versus T for Different Values for k_H/k_V.

Chapter Seven

COMPUTER PROGRAM DOCUMENTATION

The program CONS-2DFE is based on the Code FLOWCP developed by Sandhu [24] and includes some modifications.

Capabilities of the Program

The program can be used to solve problems of consolidation and drainage, foundations settlements under loads, drainage and settlement of embankments, and analyze the effectiveness of sand drains, drainage wells and drainage blankets.

The application of the program to plane strain problems may include the following features:

1. The loading of the saturated soil may be through strip footings (rigid or flexible), slabs, pavements, and embankments.
2. Anisotropic and multi-layered soil systems up to eight layers with wide variation of material properties. Greater numbers of layers may be analyzed by increasing the core storage requirements of the program.
3. Arbitrary rate of loadings and geometrical configurations.
4. Arbitrary time increment (Δt) for various periods of consolidation.

The program will generate histories of stresses, pore pressures, horizontal and vertical displacements and flow velocities.

Chapter Eight

SUMMARY, CONCLUSIONS AND RECOMMENDATIONS

Summary

The purpose of this study was to present an analysis for predicting the magnitude and rate of settlement and the magnitude of the pore water pressure during consolidation of linear elastic soils by using the finite element method. The formulation of the method is based on a variational principle.

The numerical characteristics of the method for one- and two-dimensional problems in plane strain were examined and the results were presented in graphical form to illustrate the effect of mesh refinement. Other factors examined in 2-D problems were the effect on the results of Poisson's ratio ν, the relative distance to the boundary, and the time increment.

For multilayered soil systems a parametric study was made. The effects of wide variations in material properties on the consolidation process and general criteria for reliable results using the FE formulation were derived. A three-layered system was used for the parametric study on the material parameters. The method was applied to four layer field problem and the results were found to be reasonable.

Permeability and strength anisotropy and their effect on the rate of consolidation were examined for a homogeneous soil under a strip footing.

Conclusions and Recommendations

The results of this investigation have shown that the finite element procedure is very useful in obtaining solutions for consolidation problems involving homogeneous, anisotropic and layered soil systems. On the basis of the analysis presented, the following conclusions and remarks are offered:

1. For greater engineering accuracy, a reasonably fine mesh should be used. This was observed in the one-dimensional analysis where convergence plots for various meshes of 21, 33 and 63 nodes showed that the mesh with 63 nodes produced minimum error in the pore water pressure prediction.
2. In the two-dimensional analysis, pore water pressures seem to be inaccurate at early times $T = 2.5 \times 10^{-3}$ and $T = 4.5 \times 10^{-3}$ but for later times, $T = .42$ and $T = 1.25$, the solutions are more consistent.
3. The higher the Poisson's ratio,the higher the rate of consolidation settlement.
4. The geometry of FE mesh, boundary conditions and time increment should be carefully selected for each problem. A value of dimensionless factor λ less than 5.0×10^{-3} was found to yield reliable answers.
5. For the analysis of multilayered soils, the procedure used can give satisfactory results for a wide range of material properties. Ratios of elastic modulus E_r and permeability constant k_r in the range of 1.0 to 10^5 were examined and it

was found that the results beyond ratios of $E_r = 10^3$ and $k_r = 10^4$ become irregular.

6. From the analysis of soils with strength anisotropy it was found that when $E_y > E_x$ the rate of consolidation settlement was smaller throughout the process. For $E_x > E_y$ the rate of consolidation settlement is reduced at early times and it increases at later times of the process. The solution breaks down beyond a ratio of $\frac{E_x}{E_y} > 1.7$.
7. For soils exhibiting permeability anisotropy the rate of consolidation settlement for higher horizontal permeability is accelerated at early times and it is reduced at later times of the process.

Finally, the analysis presented herein with some modifications can be easily extended to include nonlinear material properties and axisymmetric consolidation problems.

BIBLIOGRAPHY

1. Abbott, M.B., "One-Dimensional Consolidation of Multi-Layered Soils", Geotechnique, vol. 10, 1960, London, pp. 151-165.

2. Barden, L. and Younan, N.A., "Consolidation of Layered Clays", Canadian Geotechnical Journal, vol. 6, 1969, pp. 413-429.

3. Biot, M.A., "General Theory of Three-Dimensional Consolidation", Journal of Applied Physics, vol. 12, 1941, pp. 151-164.

4. Biot, M.A. and Clingan, F.M., "Consolidation Settlement of a Soil with an Impervious Top Surface", Journal of Applied Physics, vol. 12, 1941, pp. 578-582.

5. Christian, J.T. and Boehmer, J.W., "Plane Strain Consolidation by Finite Elements", Journal of the Soil Mechanics and Foundation Division, American Society of Civil Engineers, vol. 96, 1970, pp. 1435-1457.

6. Christian, J.T., Boehmer, J.W., and Martin, P.P., "Consolidation of a Layer Under a Strip Load", Journal of Soil Mechanics and Foundations Division, ASCE, vol. 98, no. SM7, 1972, pp. 693-707.

7. Cryer, C.W., "A Comparison of the Three-Dimensional Consolidation Theories of Biot and Terzaghi", Quarterly Journal of Mechanics and Applied Mathematics, vol. 16, 1963, pp. 401-412.

8. Davis, E.H., and Poulos, H.G., "Rate of Settlement under Two- and Three-Dimensional Conditions", Geotechnique, vol. 22, no. 1, 1972, pp. 95-114.

9. Desai, C.S., "Analysis of Consolidation by Numerical Methods", Proc. Symp. on Recent Developments in the Analysis of Soil Behavior and their Application to Geotechnical Structures, University of NSW, Australia, July, 1975.

10. Desai, C.S. and Johnson, L.D., "Evaluation of Some Numerical Schemes for Consolidation", International Journal of Numerical Methods in Engineering, vol. 7, 1973, pp. 243-254.

11. Desai, C.S. and Johnson, L.D., "Evaluation of Two Finite Element Formulations for One-Dimensional Consolidation", Computers and Structures, vol. 2, 1972, Pergammon Press, pp. 469-486.

12. Desai, C.S. and Abel, J.F., Introduction to the Finite Element Method, 1972, New York, Van Nostrand Reinhold Co.

13. Gray, H., "Simultaneous Consolidation of Contiguous Layers of Unlike Compressible Soils", Transactions, ASCE, vol. 110, 1945, pp. 1327-1356.

14. Gibson, R.E., Schiffman, R.L., and Pu, S.L., "Plane Strain and Axially Symmetric Consolidation of a Clay Layer on a Smooth Impervious Base", Quarterly Journal of Mechanics and Applied Mathematics, vol. 23, no. 4, 1970, pp. 505-520.

15. Hwang, C.T., Morgenstern, N.R., and Murray, D.W., "On Solutions of Plane Strain Consolidation Problems by Finite Element Methods", Canadian Geotechnical Journal, vol. 8, 1970, pp. 109-118.

16. Ladd, C.C. and Wissa, A.E.Z., "Geology and Engineering Properties of Connecticut Valley Varved Clays with Special Reference to Embankment Construction", MIT Department of Civil Engineering, Report R70-56, Sept. 1970.

17. Lo, K.V., "Stability of Slopes in Anisotropic Soils", Journal of Soil Mechanics and Foundation Division, ASCE, vol. 91, July, 1965, pp. 85-106.

18. Mandel, J., "Consolidation des Sols (Etude Mathematique)", Geotechnique, vol. 3, 1953, pp. 287-299.

19. McNamee, J. and Gibson, R.E., "Plane Strain and Axially Symmetric Problems of the Consolidation of a Semi-Infinite Clay Stratum", Quarterly Journal of Mechanics and Applied Mathematics, vol. 13, 1960, part 2, pp. 210-227.

20. Murray, T.R., "Computer Program for Multi-layer Soil Settlement", Transport and Road Research Laboratory, Civil Engineering and Public Works Review, vol. 68, Dec. 1973, pp. 1087-1089.

21.. Rendulic, L., "Porenziffer und Porenwasserdruck in Tonen", Der Bouingenieur, vol. 17, no. 51/53, 1936, pp. 559-564.

22. Sandhu, R.S., Fluid Flow in Saturated Porous Elastic Media, Ph.D. Thesis, University of California, Berkeley, 1968.

23. Sandhu, R.S., and Wilson, E.L., "Finite Element Analysis of Seepage in Elastic Media", Journal of Engineering Mechanics Division, ASCE, vol. 95, 1969, pp. 641-652.

24. Sandhu, R.S., "Strip Footing Analysis", Report to FHWA, Columbus, Ohio, April, 1972.

25. Saxena, S. Personal Communication.

26. Schiffman, R.L., Chen,A.T.F. and Jordan, J.C., "An Analysis of Consolidation Theories", Journal of Soil Mechanics and Foundations Division, ASCE, vol. 95, no. SM1, 1969, pp. 285-312.

27. Schiffman, R.L. and Gibson, E.R.,"Consolidation of Non-homogeneous Clay Layers", Journal of the Soil Mechanics and Foundation Division, ASCE, vol. 90, 1964, pp. 1-30.

28. Schiffman, R.L. and Stein, J.R.,"One-Dimensional Consolidation of Layered Systems", Journal of Soil Mechanics and Foundation Division, ASCE, vol. 96, no. SM4, July, 1970, Proc. Paper 7387.

29. Skempton, A.W. and Bjerrum, L., "A Contribution to Settlement Analysis of Foundations On Clay", Geotechnique, vol. 7, 1957, pp. 168-178.

30. Taylor, D.W., Fundamentals of Soil Mechanics, John Wiley and Sons, Inc., New York, 1964, pp. 224-234.

31. Tergazhi, K. and Peck, R.B., Soil Mechanics in Engineering Practice, John Wiley and Sons, Inc., New York, 1968.

32. Valliappan, S., Lee, I.K., and Boonlualohr, P. "Finite Element Analysis of Consolidation Problem",Proc. Symp. Finite Element Methods in Flow Problems, Oden, J.T., et al (editors), UAH Press, Swansen, U.K., 1964, pp. 741-755.

33. Yokoo, Y., Yamagata, K., and Nougaota, H.,"Finite Element Method Applied to Biot's Consolidation Theory", Soils and Foundations, Japanese Society of Soil Mechanics and Foundation Engineering, vol. 11, no. 1, 1971, pp. 29-46.

34. Zienckiewicz, O.C., and Cheung, Y.K., The Finite Element Method in Structural and Continuum Mechanics, McGraw-Hill, London, England, 1967.

VITA

Spelios A. Asproudas was born in Patras, Greece, on August 29, 1948. He was graduated from the A! Lyceon of Patras in 1965 and in 1966 he attended Phillipsburg High School, Phillipsburg, New Jersey, where he received a certificate of achievement. In 1967, he entered West Virginia Institute of Technology, Montgomery, West Virginia, where he graduated with a Bachelor's of Science in Civil Engineering in May of 1971. He then joined the West Virginia Department of Highways, where he worked as a highway design engineer until July of 1973. September of 1973, he began graduate studies at Virginia Polytechnic Institute and State University in pursuit of the degree of Master of Science in Civil Engineering.

Spelios A. Asproudas

FINITE ELEMENT ANALYSIS FOR CONSOLIDATION OF MULTILAYERED AND ANISOTROPIC SOILS

by

Spelios A. Asproudas

(ABSTRACT)

The problem of consolidation for multilayered and anisotropic, linear elastic soils was investigated. The finite element method was used for the analysis. The numerical characteristics of the method for one- and two-dimensional problems in plane strain were examined. The effect of wide variations in material properties of multilayered soil systems on the consolidation process and quantitative criteria for reliable results were derived. Permeability and strength anisotropy and their effect on the rate of consolidation were examined for a homogeneous soil under a strip footing. The method was applied to a four-layered field problem and the results were found to be reasonable.